UNIVERSITY OF CALIFORNIA SAN DIEGO

Insights Into the Mechanism of Signal-Induced IKK Activation

A Thesis submitted in partial satisfaction of the requirements
for the degree Master of Science

in

Chemistry

by

Kyle Toyojiro Shumate

Committee in charge:

Professor Gourisankar Ghosh, Chair
Professor Rommie Amaro
Professor Elizabeth Komives

2019

The Thesis of Kyle Toyojiro Shumate is approved, and it is acceptable in quality and form for publication on microfilm and electronically:

_____

_____

_____
Chair

University of California San Diego

2019

DEDICATION

I dedicate this to my fiancé Jordy who has been my greatest support to lean on throughout this journey and my dog Cosmo who is an amazing Pembroke Welsh Corgi.

TABLE OF CONTENTS

LIST OF ABBREVIATIONS

ARD	ankyrin repeats domain
BME	β-mercaptoethanol
DD	dimerization domain
DTT	dithiothreitol
ECL	enhanced chemiluminescence
IκB	inhibitor of NF-κB
IKK	inhibitor of NF-κB kinase
IPTG	isopropyl β-D-1-thiogalactopyranoside
kDa	kilodalton
MW	molecular weight
NEMO	NF-κB essential modulator
NF-κB	nuclear factor kappa B
NLS	nuclear localization sequence
NTA	nitrilotriacetic acid
NTD	N-terminal domain
PAGE	polyacrylamide gel electrophoresis
PEST	sequence rich in Pro, Glu, Ser and Thr
PIC	protease inhibitor cocktail

PMSF	phenylmethylsulfonyl fluoride
RHR	Rel homology region
Sf9	*Spodoptera frugiperda* 9
SDS	sodium dodecyl sulfate
TAD	transcriptional activation domain

LIST OF FIGURES

ACKNOWLEDGEMENT

Thank you to Professor Gourisankar Ghosh for giving me the opportunity to conduct research and pursue my dreams of being a scientist. I appreciate the hard work ethic and persistence you've inspired in me. I have learned a lot about myself from working in your lab. I felt that I've grown in skill and confidence as a researcher. I have learned so much from working for you and I am forever grateful.

Thank you Professors Elizabeth Komives and Rommie Amaro. I am inspired by your accomplishments in research. It has been amazing to learn from both of you. Thank you very much for taking the time to evaluate my thesis.

Thank you Samantha Cohen for teaching me proper techniques as an undergraduate student. As a mentor you've been very generous in assigning me roles in the project to determine insights into IKK activation. I am grateful for your contribution to our research. It has definitely been enjoyable working together on this project.

Thank you Myung Soo Ko for working together with me to resolve the NEMO-IKK2/β complexes by size exclusion chromatography and SDS-PAGE. Thank you for getting me hooked on ramen, which has been a lifesaver on tough days.

Thank you Tapan Biswas for teaching me valuable NGC techniques and giving constructive criticisms which have been immensely useful. My projects have found success because of your tremendous analytical skills and technical expertise.

Thank you Mari Carmen Muerlo for teaching me all about Electromobility Shift Assay. You are one of the most friendly people I have come to know.

Thank you to all Gourisankar Ghosh Lab members past and present for all your contributions to the lab. Thank you for your contributions to research and protocols.

ABSTRACT OF THE THESIS

Insights Into the Mechanism of IKK Activation

by

Kyle Toyojiro Shumate

Masters of Science in Chemistry

University of California San Diego, 2019

Professor Gourisankar Ghosh, Chair

NF-κB transcription factors are essential for inflammation, proliferation, survival, growth and differentiation. The exact mechanism for NF-κB activation by IKK phosphorylation is not well understood. However, it is well known that the partners IKK1/α, IKK2/β, NEMO and Linear Ub_n chains are essential for IKK activity. Moreover, phosphorylation of serines 177/181 is a key event in IKK activation, which can be performed by upstream kinases or trans-

autophosphorylation by IKK2/β. We confirmed previous results which showed that IKK2/β-NEMO will form a higher molecular weight complex in size exclusion chromatography and we show that Ub_4 can bind sub-stoichiometrically to this complex. In addition to an established IKK2/β-NEMO interacting domain we discovered a secondary site of interaction between IKK2/β and the 339 to C-terminal region of NEMO that is Ub_4 dependent. We propose that IKK complex oligomerizes and this higher order structure requires both IKK2/β and NEMO to oligomerize. Moreover, since Ub_4 is essential for trans-autophosphorylation, (IKK activation), the binding of Ub_4 to oligomerized NEMO-IKK2/β may induce a conformational change which allows for IKK trans-autophosphorylation. IKK2/β-NEMO interaction through a secondary site, mediated by Ub_4, may have a pivotal role in trans-autophosphorylation.

I. Introduction

The NF-κB and IκB proteins

NF-κB refers to a family of dimeric transcription factors that are generated from five protomers [1]. These protomers are p50, p52, p65(RelA), cRel and RelB. NF-κB factors share a highly conserved region called Rel homology region (RHR) which is essential for NF-κB dimerization, nuclear localization and DNA binding. RelA (p65) and p50 heterodimers are the most common type of NF-κB found in all cells [1].

All NF-κB dimers are kept inactive in the cytosol by inhibitor of NF-κB (IκB) family of proteins. IκB proteins bound to NF-κB dimers will mask the nuclear localization signal in the RHR [12]. There are five IκB family inhibitors that shown overlapping but distinct NF-κB binding specificity. One of these IκB proteins, IκBα, is bound to RelA (p65) and p50 NF-κB heterodimer.

A large number of extra or intra-cellular stimuli induces rapid NF-κB translocation to the nucleus through removal of IκB. This results in expression of a large array of genes downstream of κB sites and many physiological responses such as inflammation, immunity, cell death and proliferation [1, 2]. Upstream signals which initiate activation are tightly regulated yet need to be specific to initiate the correct physiological response in the cell [12]. Aberrant NF-κB activation results in many diseases, immune dysfunction and irregularities [16, 17, 18, 28].

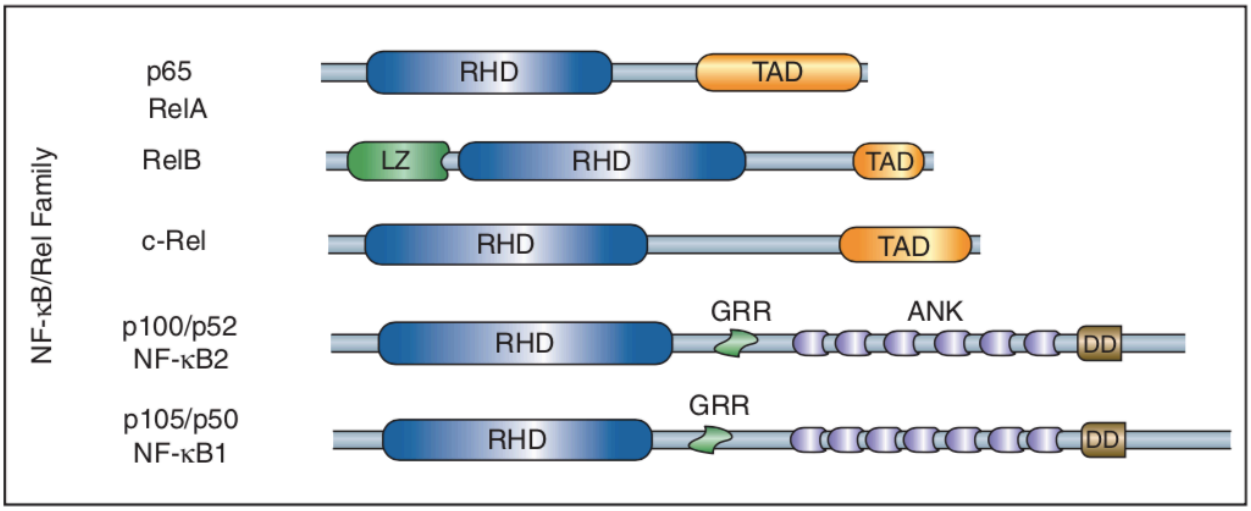

Figure 1. NF-κB Protomer Family. RHD = Rel homology domain; TAD = transcription activation domain; GRR = glycine-rich regions; ANK = ankyrin repeats; DD = death domain.

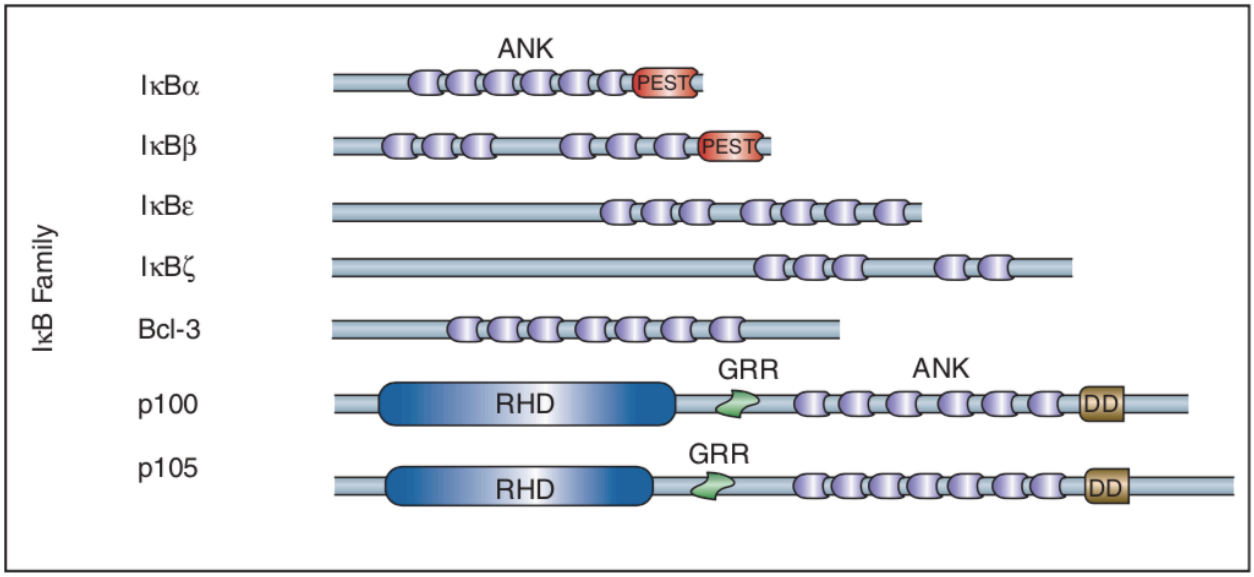

Figure 2. IκB Protein Family. ANK = ankyrin repeats, PEST = proline/glutamic acid/serine/threonine-rich sequence. Scheidereit, C. et. al. (2006).

Canonical NF-κB signaling

Upstream signals orchestrate a series of reactions leading to NF-kB activation. The signaling pathways that actives p50:RelA heterodimer is known as canonical signaling. The key point of canonical signaling is the activation of protein kinase known as Inhibitor of κB Kinase (IKK). The IKK is a trimeric complex composed of IKK1/α, IKK2/β and NEMO (NF-κB Essential Modulator) [4-8]. The most well-characterized IKK activation pathways is the one activation by cytokines such as TNFα (tumor necrosis factor alpha). TNF-α, a pleiotropic inflammatory cytokine trimer, binds to TNFR-1 on the cell membrane and induces TNRFR-1 trimer formation [12]. This recruits the first complex composed of TRADD, RIPK1, TRAF2 which recruit c-IAP1 and c-IAP2. These are E3 ligases which polyubiquitinate RIPK1 with K11 and K63 Ub chains. This event recruits the E3 ligase LUBAC, which polyubiquitinates RIPK1 and c-IAPs with M1 linked Ub chains [12, 40]. Polyubiquitinated RIPK1 attracts IKK and LUBAC polyubiquitinates NEMO with M1-linked poly-Ub chains. Polyubiquitinated RIPK1 also attracts TAK1 complex which induces autophosphorylation and activation of TAK1. This may setup an optimal proximity for TAK1 mediated IKK activation by phosphorylation of the activation loop serine^{177} on IKK2/β [12, 40].

In the case of TNFα-induced IKK activation, Met1 Ub-chain formation is critical. The Met1 Ub-chain is covalently linked to the adapter NEMO subunit of the IKK complex. The covalently-linked Met1 Ub-chain also makes non-covalent interactions with NEMO. These processes ultimately activate the catalytic IKK2/β subunit of the IKK complex. The precise mechanism of how IKK2/β undergoes activation is the main focus of my thesis.

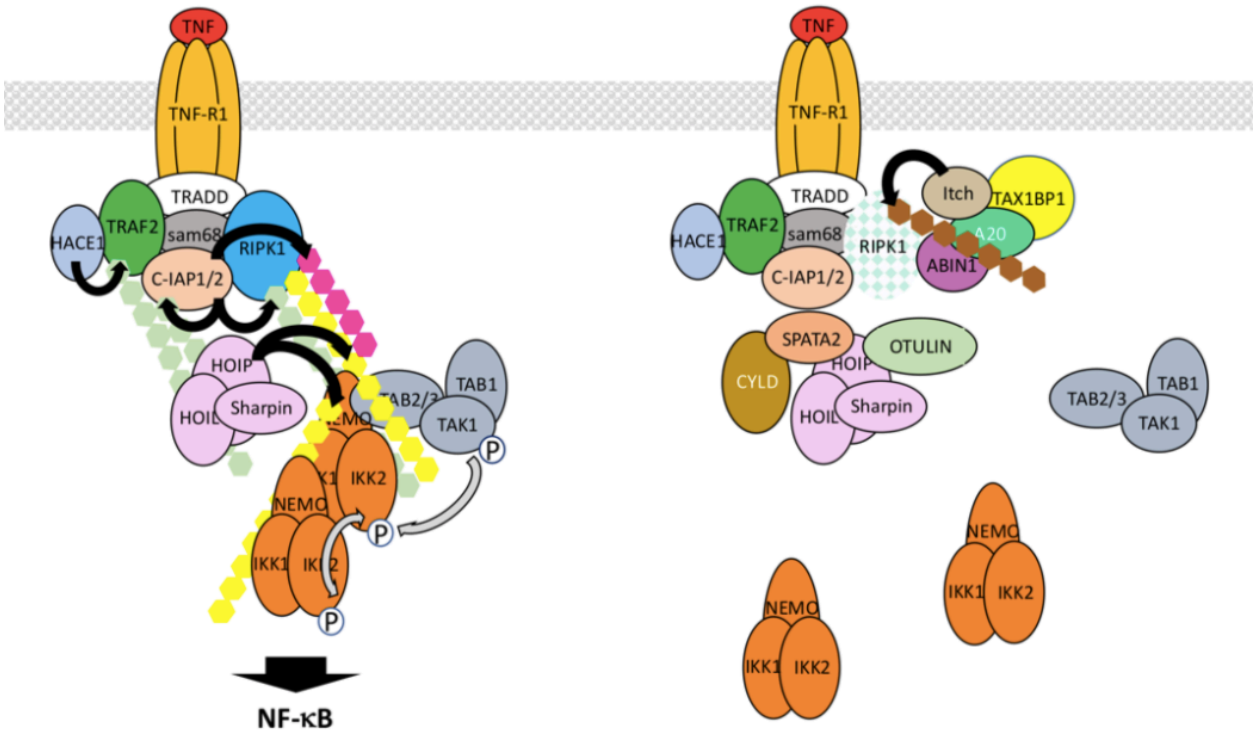

Figure 3. TNF-R1 Signaling Pathway. Canonical activation of IKK through the TNF-R1 signaling pathway. M1-, K11- and K63 linked polyubiquitin chains are indicated by yellow, pink and green hexagons. Inhibitors of IKK activation are shown on the right side of the panel. (Courtois and Fauvarque, 2018).

The IKK Complex

The catalytic IKK1/α and IKK2/β proteins are over 700 amino acids long kinases which bear over 50% sequence homology. The domain architectures of these kinases are also very similar. The kinase domain (KD) is located at the N-terminus followed by a ubiquitin-like domain (ULD) and ends with a third folded domain referred to as the scaffold dimerization domain (SDD). The SDD is a long triple helical fold that binds to the KD and ULD at its N-terminal half and dimerizes through the C-terminal half. The C-terminal ~80 residues form a flexible segment that is responsible for high affinity interaction with NEMO. Hence this region is known as the NEMO binding domain (NBD). The structure of IKK1/α and IKK2/β dimers are known [29, 41]. Mutational experiments have shown that interactions between KD and SDD or ULD and SDD are important for the catalytic activity of KD.

NEMO is coiled coil (CC) protein in most part barring the extreme N and C-termini. The N-terminal CC region (40-110) is responsible for NEMO binding followed by another CC segment (111-250) of unknown function. The third CC region (251-360) is known as CC-LZ because of the existence of periodic leucines. The CC-LZ region is responsible for non-covalent Ub-chain binding. As indicated earlier, this non-covalent interaction between NEMO and the Met1 Ub chain is essential for IKK2/β activation. Met1 Ub chain binds over 100-fold more tightly than the K63-linked Ub chain. T The C-terminus (389-419) contain a zinc-finger domain which is preceded by a short polyproline segment (265-285). NEMO does two critical functions- it connects upstream signal to IKK2/β and plays a role in substrate binding for phosphorylation. The primary substrate of the IKK complex is IkBa:p50:RelA complex. Two serines located at the N-terminus of IkBα, Ser32 and Ser36, are phosphorylated by the IKK2/β subunit of the IKK complex. Upon phosphorylation, IκBα is ubiquitinated with K48 linked Ub chains and degraded

by the proteasome leading to release of NF-κB [1, 2, 3]. Free NF-κB then can bind DNA response elements of hundreds of genes to regulate their expression.

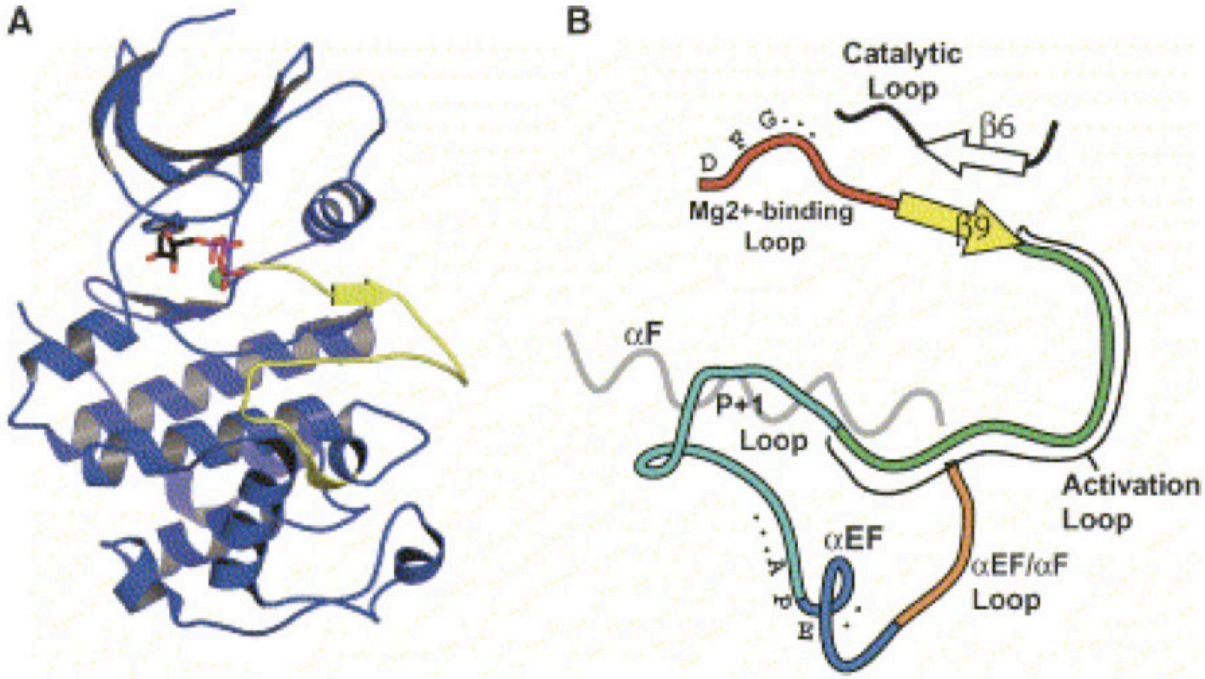

Figure 4. Active Loop Motif of Signal Transduction Kinases. (Nolen et al., 2004)

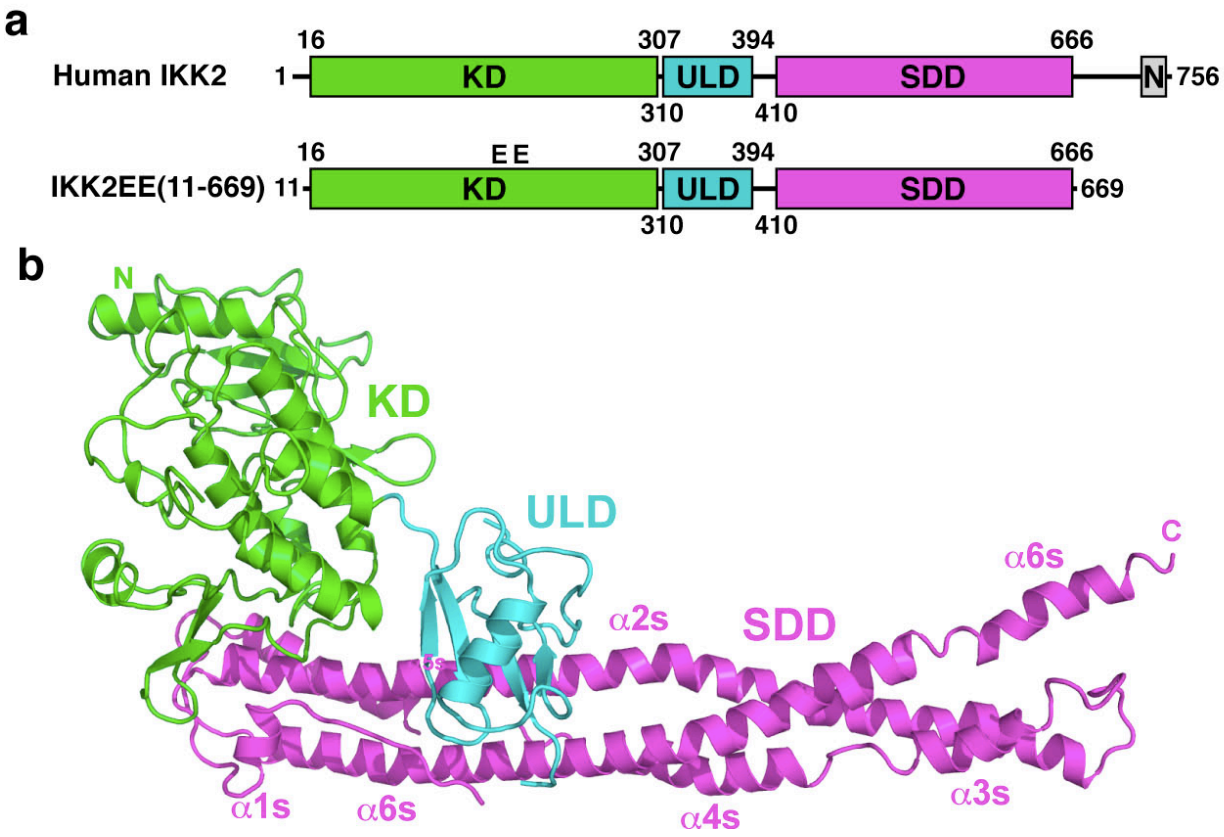

Figure 5. Human IKK2 Crystal Structure. (Ghosh et. al., 2013)

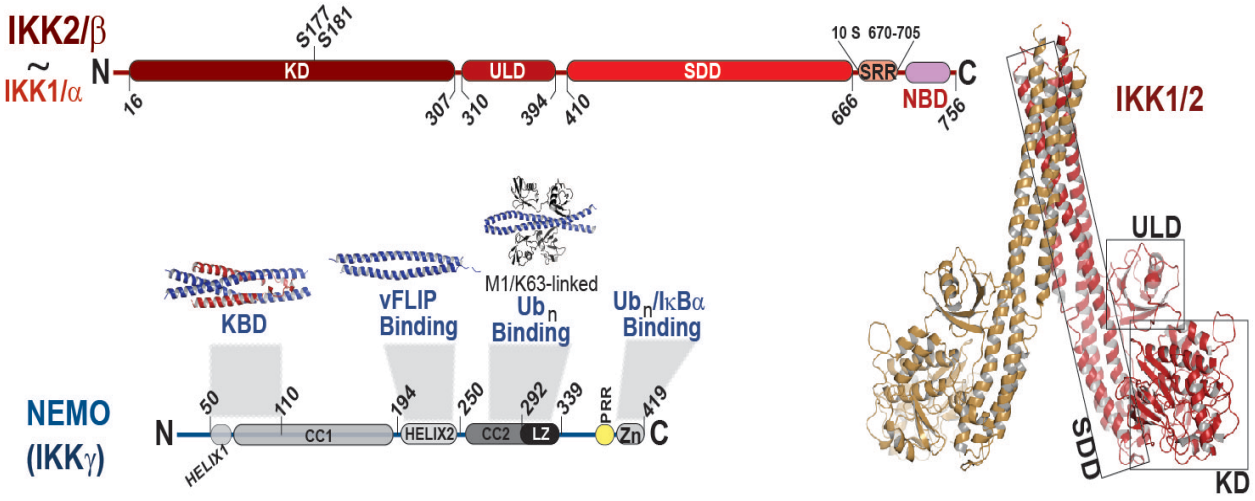

Figure 6. Depiction of IKK1, IKK2 and NEMO domain architecture. Theoretical structure of IKK1/2 heterodimer composed of published crystal structures [29, 41].

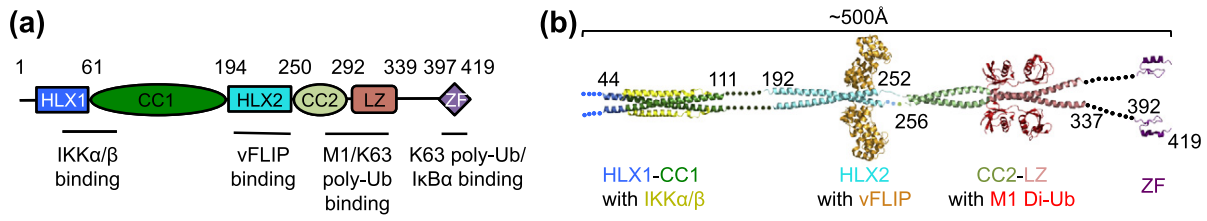

Figure 7. Partial Crystal Structures of NEMO with Adaptor Proteins. [21, 30, 42, 43].

A working model of IKK2/β activation

The activation of IKK2/β means phosphorylation of its two serines, Ser177 and Ser181, in the activation loop (AL). Hence, the IKK2/β phosphomimetic mutant (Ser177Glu/Ser181Glu) is constitutively active bypassing the requirement of signaling [41].

Activated IKK complex can also trans-autophosphorylate other IKK complexes (Ser177 and Ser181 of IKK2/β) [32, 34, 40]. This is evident from phosphorylation, hence activation, of IKK2/β *in vitro* when incubated with NEMO and unanchored Ub_n chains [19, 26]. LUBAC polyubiquitinated NEMO *in vitro* has also been shown to enhance IKK trans-autophosphorylation better than NEMO incubated with unanchored polyubiquitin chains [27]. Moreover, IKK activation can occur in cells with overexpressed IKK2/β. This may indicate that proximity between neighboring IKK2/β molecules is important factor to activate IKK2/β through trans-autophosphorylation.

In unstimulated cells these serines remain in a state that cannot be phosphorylated and/or a kinase that is responsible for Ser177/181 phosphorylation remains inactive. It is generally thought that the K63 Ub-chain recruits and activates TAK1, an upstream IKK kinase. The Ub-chain-mediated clustering of TAK1 or other upstream kinases, and IKK2/β allows these upstream kinases to phosphorylate the activation loop (AL) loop of IKK2/β directly. While both Met1 and K63 Ub-chains play essential roles in IL-1β signaling, the latter is not required for TNFα signaling. Interestingly, unanchored Met1 Ub-chains can interact with NEMO to activate IKK2/β. These results suggest that Met1 Ub-chains are critical for most if not all canonical signaling whereas other Ub-linkages play signal-specific roles. Several reports suggested IKK2/β can activate itself by autophosphorylation *in trans*. A recent report showed that TAK1 phosphorylates Ser177 whereas Ser181 undergoes autophosphorylation in trans. While the

essential roles of Ub-chains in IKK2/β activation are becoming clear, how these chains play a direct IKK proximal role in IKK activation is less clear. Also unknown is the IKK-intrinsic events during the Ub-chain dependent activation process. For instance, the ALs of all signaling kinases maintain structural states that might not be accessible to an upstream kinase. Therefore, a conformational switch program should be in place as part of the signaling pathway.

The IKK2/β structure determined in our laboratory enabled us to develop a model of transient oligomerization-dependent IKK2/β activation (**Fig. 8**). In the crystal, IKK2/β forms several distinct protein-protein interfaces. We tested these interfaces and found that they are functionally important. We are particularly intrigued by the 'V-shaped' tetrameric interface (hereafter 'V-surface') [31]. We now have evidence suggesting that this interface is possibly involved in communicating with the upstream signal (discussed below). Interestingly, a small pool of IKK1/α formed a hexameric scaffold arising from trimeric arrangements of the dimers (**Fig. 9**). Mutations disrupting the IKK1/α trimer interface reduced its binding to NIK, affecting the non-canonical signaling but not canonical signaling mediated by IKK2/β [41]. Curiously, the 'V-surface' of IKK2/β and the trimeric interface of IKK1/α map at equivalent locations further suggesting their functional significance [31, 41].

The structure of this entire complex in its resting or active state has not been explicitly shown before. The following results may shed some light on a possible structure of the NEMO and IKK2/β complex primed for trans-autophosphorylation.

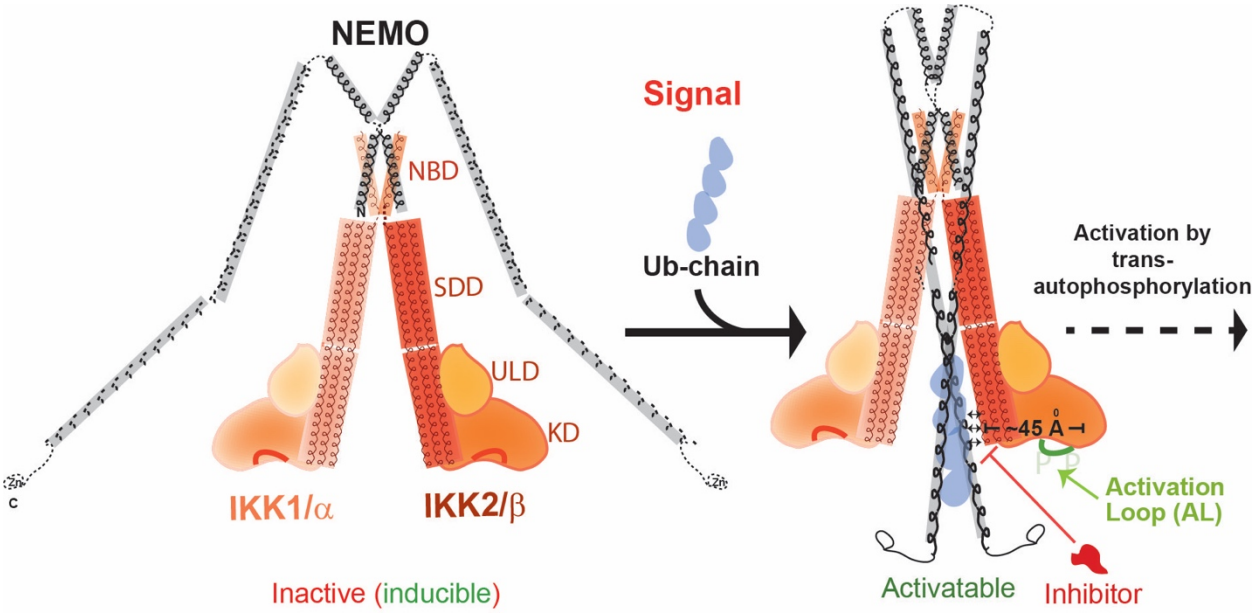

Figure 8. Proposed Model of Transient Oligomerization Dependent IKK Activation. Activation loop is proposed to undergo a conformation change due to allosteric interactions of IKK2/β and NEMO bound to polyubiquitin chains.

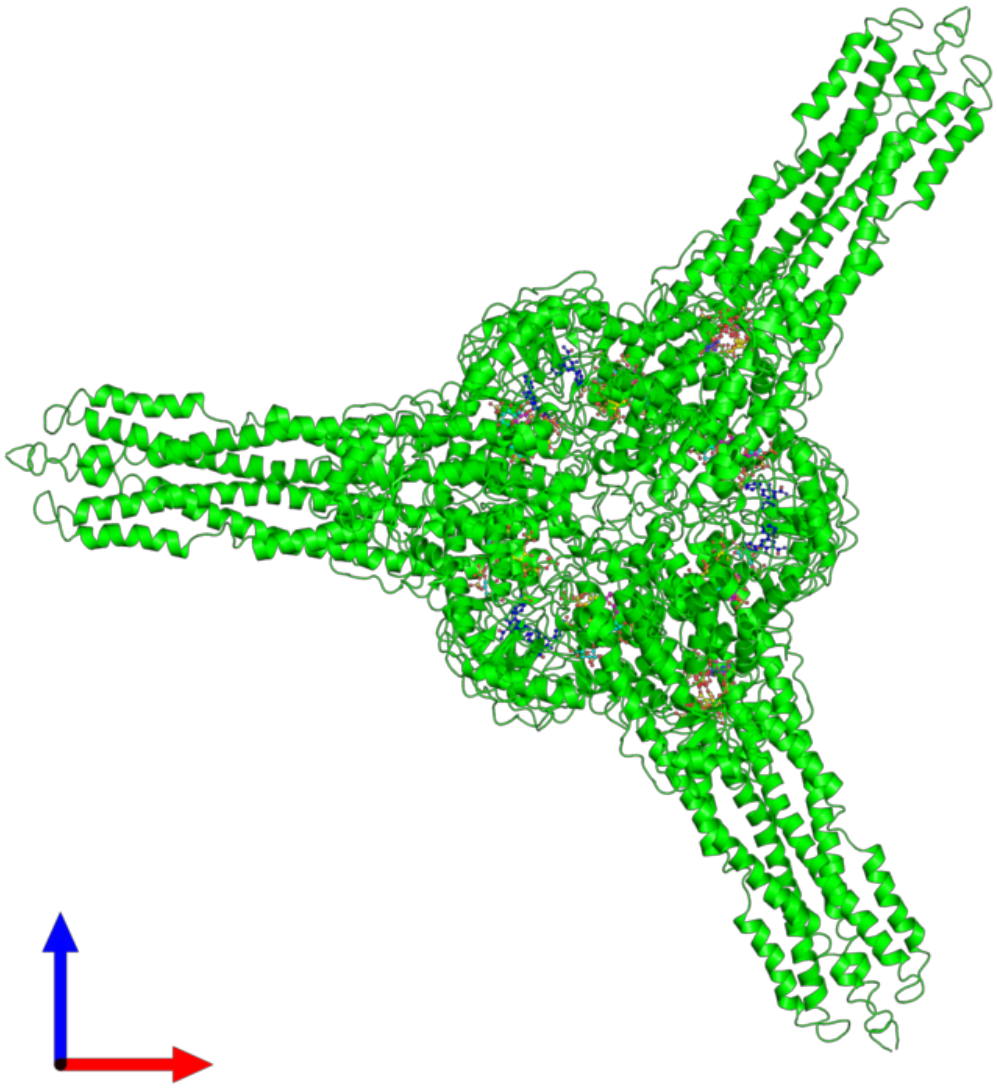

Figure 9. Hexameric Scaffold of IKK1/α Arising from Trimeric Arrangement of Dimers. (Polley et al., 2016).

Focus of my thesis

I proposed a hypothesis that Met1 Ub-chain covalent conjugated to NEMO that also binds non-covalently to the CC-LZ domain of NEMO induces a conformational change in NEMO which allows NEMO to transiently bind to SDD of IKK2/β. I also propose that the transient interaction site on SDD involved the V-interface observed in the crystal structure of IKK2/β performed in our laboratory. This transient interaction induces conformational change of the AL located at the opposite site. The serines (Ser177 and Ser181) now can be phosphorylated by an upstream kinase or by itself through autophosphorylation.

II. Materials and Methods

A. Insect Cell Protocols

1. Generating Baculovirus for His_6-IKKβ Protein Expression

His_6-IKKβ constructs were previously cloned into pFastBac Htb (Invitrogen) [32]. Chemically competent DH10B *E. coli* were transformed with pFASTBac Htb IKKβ constructs and spread onto LB agar plates with freshly added gentamycin, kanamycin, IPTG and 5-bromo-4-chloro-3-indolyl-β-D-galactopyranoside (X-gal, Sigma). DH10B plaques which appeared white in color were touched with sterile wire loops and spread onto LB agar plates. Streaked clones which were completely white in appearance (in comparison to blue negative controls) were picked to inoculate 5-10 mL of SOB broth.

Cultures were centrifuged and then Bacmid DNA extracted (Accuprep Plasmid Mini Extraction Kit) for transfection in SF9 cells. 1 μg of Bacmid DNA was mixed with 250 mL of Sf9 media (free of serum and PSG) and 3 μL of PEI. The Bacmid DNA, PEI and Sf9 media mixture was incubated at room temperature for 30 minutes. Meanwhile, 0.8 $x10^6$ Sf9 cells were allowed to attach to a 2.5 cm TC dish for 30 minutes. After cells had attached to the dish, the media was removed and fresh Sf9 media free of serum/PSG was layered on top. The mixture of Bacmid DNA, PEI and Sf9 media was added dropwise to the Sf9 cells in the TC dish. The transfected Sf9 cells were cultured at 27°C for 96 hours to generate P1 virus.

Media containing the P1 virus was removed from the culture dish and stored in sterile microcentrifuge tubes at 4°C. In a 6 well TC plate, the P1 virus was added to 0.8 $x10^6$ adhered Sf9 cells in 2 mL of Sf9 media per well. Five dilutions of the virus ($1/10^{th}$, $1/15^{th}$, $1/25^{th}$, $1/50^{th}$, $1/100^{th}$ of 2 mL) were tested and compared to the uninfected control. After 72-96 hours the media was removed and the P2 virus was stored in falcon tubes at 4°C. The Sf9 cells were washed with cold DPBS, removed from the TC plates by pipetting, pelleted in microcentrifuge

tubes and lysed with RIPA buffer. The expression of recombinant protein was analyzed by western blot with IKK2/β antibody.

To generate P3 virus, 22 x10^6 Sf9 cells adhered to a 15 cm TC dish were infected with the P2 virus and dilution volume correlated with the best IKK2/β expression. After 72-96 hours the media was removed to a 50 mL falcon tube and stored at 4°C. In order to freeze the virus, media was supplemented with 10% FBS and 10% DMSO.

2. Large Scale Sf9 Infection with IKK2/β Baculovirus

Sf9 cells were cultured in ESF 921 Insect Cell Culture Media (Protein Free). Sf9 cell density was maintained between 1-3 x10^6 cells per milliliter, which required dilution or doubling of volume every 24 hours. Sf9 culture was increased from an initial 10 mL (125 mL flask) to 330 mL (1.0 liter flask). Once density reached 2 x10^6 cells per mL the Sf9 culture was infected with the selected dilution of baculovirus (for example, a 1/100 dilution required the addition of 3.3 mL of P3 baculovirus to the 330 mL Sf9 culture). The infection proceeded for 72 hours at 27°C, on a 175 rpm shaker.

3. Sf9 Cell Lysis

Sf9 cells were lysed following previously described methods [32].

B. E. coli Cell Protocols

1. Plasmid DNA Extraction

DH5α were transformed with plasmids and previously spread on LB agar plates. After 18-30 hours of growth colonies were picked with sterile metal loops to inoculate 4 mL of LB broth with the appropriate antibiotic selection. These cultures grew for 12-16 hours before being centrifuged. Plasmid DNA to be used for transformation in Rosetta cells, PCR amplification or endonuclease digestion was extracted with the alkaline lysis protocol. Plasmid DNA to be used for transfection were extracted with the Bioneer spin column extract kit.

For large-scale extraction of plasmid DNA, a modified and scaled-up alkaline DNA extraction method for 1 liter cultures was utilized. The only major modification to the maxiprep plasmid DNA extraction protocol was as followed; plasmid DNA was precipitated by isopropanol, pelleted, resuspended in Tris-EDTA buffer and incubated with 50 μg/mL RNase A for 30 min. This plasmid DNA was precipitated and pelleted by PEI/2.5 M NaCl. The PEI/NaCl supernatant was aspirated and then the pellet was resuspended in autoclaved MilliQ H_2O.

All DNA concentrations were measured by NanoDrop.

2. Protein Expression in *E. coli*

E. coli $BL21^{Rosetta}$ cells were transformed with NEMO constructs cloned into pGEX 4T-2 via the BamHI and NotI restriction sites. Either 2 Liters of LB broth was inoculated with a 10 mL starter culture. Large scale cultures were shaken at 37°C for 2 – 4 hours till OD_{600} reached 0.5 – 0.6. Cultures were induced with 0.4 μM IPTG for 3 hours at 37°C, centrifuged at 3000 rpm for 30 min and the pellet stored in -20°C.

3. *E. coli* cell lysis

Frozen *E. coli* Rosetta pellets were thawed and resuspended in chilled lysis buffer (20 mM HEPES-KOH pH = 7.6, 300 mM potassium acetate, 20% glycerol, 10 mM magnesium chloride, 25μM $ZnSO_4$, 0.1 mM phenylmethylsulfonyl fluoride (PMSF), 5 mM β-Mercaptoethanol.) After dispensing the resuspended cells in a stainless steel graduated cylinder, stored on packed ice, the cells were sonicated with the following conditions. 1 minute 90% duty cycle and power setting 9 with 5 minutes rest on ice. Followed with 1 minute sonication with identical settings and 10 minutes rest on ice. A third sonication for 1 minute, 10 minutes rest on ice and finished with a fourth sonication. The lysate was centrifuged at 15,000 rpm for 50 minutes at 4°C.

C. Cloning and Mutagenesis

PCR fragments of NEMO constructs were generated using Pfu enzyme. PCR fragments were purified with Bioneer PCR extraction kits. NEMO PCR constructs were cloned into pGEX 4T-2 (maxiprep DNA) with BamHI and NotI Endonucleases (NEB).

Cloning NEMO-Ub_4 fusion gene required a few steps. PCR fragment of NEMO was cloned into pET28b with NdeI and BamHI endonucleases. After PCR clone screening and Plasmid miniprep the NEMO positive clones were digested with BamHI and NotI-HF. Ub_4 fragment was digested from pET24b-TetraUb vector with BamHI and NotI-HF as well. After purification the Ub_4 fragment was ligated with pET28b-NEMO with T4 ligase.

D. Protein Purification Protocols

1. Glutathione column chromatography

The clarified lysate was loaded onto equilibrated 2-3 mL of glutathione resin at a flow rate of 0.5 mL/min. After the majority of the lysate had flowed through, the lysate remaining above the resin was drained from the column. 100 mL of lysis buffer at a flow rate of 0.5 mL/min was used to wash contaminant proteins from resin. GST-tagged proteins were eluted with 25 mM Tris pH 7.5, 10 mM reduced glutathione (prepared fresh) at a flow rate of 0.5 mL/min. The elution fraction's purity were analyzed by SDS-PAGE and protein bands were visualized with Coomassie Brilliant Blue G-250 (Sigma).

For elution fractions with a relatively high concentration of contaminating proteins (see Figure 10) the elution fractions were pooled and purified by gel filtration. Superdex 16/60 120 mL column.

2. Nickel-NTA column chromatography

His_6-NEMO and His_6-Ub_4 Rosetta cells were lysed in buffer containing 250mM NaCl, 25 mM Tris pH 8.0, 10 mM Imidazole, 5 mM β-Mercaptoethanol, 0.1 mM PMSF. The clarified lysate was loaded onto 1mL of equilibrated Ni-NTA resin (BBL) at 1 mL/min. After lysate flowed through the column was washed with 500 mL wash buffer (lysis buffer + additional 10 mM Imidazole). Wash buffer was allowed to completely exit the column. Then cold elution buffer (lysis buffer + 240 mM additional Imidazole) was added in a series of 1 mL elutions fractions. These fractions were collected in microcentrifuge tubes and assayed for protein concentration/purity.

3. Nickel-NTA batch binding

Clarified His_6-IKK2/β Sf9 lysate (approximately 35 mL for a 330 mL culture) rotated at 4°C with 330 µL equilibrated Ni-NTA resin for 3 hours. This was proceeded by centrifugation (3000 rpm, 10 min). Flow through was saved in 50 mL falcon tube. The undisturbed resin was gently resuspended and moved to a 2 mL microcentrifuge tube. 8-10 washes were performed with the following conditions; addition of 1.0 mL wash buffer, rotation for 1 min at 4°C, centrifugation for 1 min at 3000 rpm and then supernatant (wash) was aspirated. The wash was saved and 20 µL of wash solution mixed with Bradford reagent. The washes were stopped when the Bradford reagent appeared the same color as the control Bradford reaction.

His_6-IKK2/β was eluted with 200 mM NaCl, 25 mM Tris pH 8.0, 10% Glycerol, 5 mM β-Mercaptoethanol, 250 mM Imidazole buffer. 330 µL of elution buffer rotated with resin at 4°C for 30 minutes. This was centrifuged and the elution fraction separated from the resin. A total of three elution fractions were collected.

E. *In vitro* Assays

1. Glutathione S-Transferase Pulldown Assays

Binding buffer was composed 150 mM NaCl, 0.5% Triton X-100, 0.5% NP-40, 10% Glycerol, 25 mM Tris-HCl pH 7.5 chilled to 4°C. Equilibrated 250 µL of Glutathione resin (BBL) in 10 mL of 100 µg/mL BSA overnight (12-16 hours).

Purified proteins were stored in 50% glycerol at -20°C. Prepared binding assays in microcentrifuges stored on ice; added proteins to a total volume of 150 µL with 2x Pulldown buffer and chilled MilliQ water. Mixed binding assay and then saved 5 µL for input SDS-PAGE and immunoblotting. Aspirated blocking buffer from glutathione resin. Added pulldown buffer to resin to bring volume to a total of 2.5 mL for 250 µL of Glutathione resin. Resuspended resin in pulldown buffer before aliquoting 150 µL to each GST reaction mixture. Total volume approximately 295 µL. Rotated GST binding assays at 4°C overnight (12-16 hours). Washed three times with pulldown buffer. Aspirated supernatant without disturbing resin, then boiled resin with 20 µL of 4XSDS-PAGE loading buffer (cold spring harbor) for 5 minutes. Loaded 2 µL of elution samples in 10% SDS acrylamide gels for GST and Ubiquitin western blot analysis. Loaded remaining (approximately 30 µL) of boiled elutions in a second 10% SDS acrylamide gel for IKKα/β western blot. SDS-PAGE electrophoresed at 130V for 25 min (till bromophenol blue reached resolving portion of SDS acrylamide gel) and 180 V for 50 min till bromophenol blue exited the bottom of the SDS acrylamide gel.

2. Superose6 10/300 resolution of NEMO, IKK2/β, Ub_4 and IκBα complexes

BioRad NGC column was setup following the manufacturer's instructions. Superose6 10/300 column was equilibrated with filtered buffer, (250 mM NaCl, 25 mM Tris pH 8.0, 10% glycerol, 2 mM DTT, chilled to 4°C). To form the NEMO:IKK2/β complexes, purified proteins

were added to a binding mixture for a total volume of 250 µL and rotated at 4°C for 1 hour. Binding mixture was filtered and then injected into 200 µL loop. After sample was loaded onto the column, the complex was eluted at a rate of 0.200 mL/min and collected in 0.333 µL fractions. Determination of the void volume with blue dextran followed identical settings but experiment was performed at RT instead of 4°C.

36 µL of fractions was boiled with 4X SDS loading dye, centrifuged, loaded onto 18 well 10% SDS acrylamide gels, electrophoresed, stained with Coomassie Brilliant Blue G-250 solution and then destained.

To determine the relationship between molecular weight and retention volume I had to calculate the average equilibrium coefficient (K_{av}) for each protein in the molecular weight standard. K_{av} was determined from the total geometric volume of the Superose6 10/300 column (V_C), void volume as determined by blue dextran (V_0) and the retention volume of the eluted protein (V_E):

$$K_{av} = \frac{(V_E - V_0)}{(V_C - V_0)}$$

The logarithm of molecular weight (Da) was plotted against K_{av} to determine a linear relationship between molecular weight and retention volume.

F. Western Blot

For transferring the protein to PVDF, acrylamide gels were rinsed in Semi-dry transfer buffer, PVDF membrane dipped in 100% methanol solution for 1 minute. Created a sandwich with the blotting paper, PVDF membrane and acrylamide gel then gently rolled the sandwich 25 times to remove air pockets. BioRad semi-dry transfer apparatus. 25 V for 80 min. Blocked PVDF membranes with 3% BSA in 1X TBST for 1 hour at room temperature. Incubated membranes with primary antibodies (1:2,000 dilution and 1:20,000 for Ubiquitin primary antibody) at 4°C on shaker overnight (18-24 hours). Poured off primary antibody solution, washed membranes 3 times for 10 minutes with 1X TBST buffer. Incubated membranes with secondary antibody (1:10,000 dilution) for 1 hour at RT (22°C) on shaker. Washed membrane 3 times for 10 minutes with 1X TBST buffer.

For visualization in ChemiDoc (BioRad); rinsed membranes with autoclaved RT MilliQ H_2O. Placed membranes on clear plastic sheet and added ECL reagent (10 mM Tris pH 8.8, Luminol, p-Coumaric acid, hydrogen peroxide) as described before [39]. Gently agitated plastic sheet to spread reagent around evenly. After 90 seconds, poured off ECL reagent, rearranged membranes with plastic tweezers to the correct alignment and covered membranes with plastic wrap. Exposed membranes in ChemiDoc using identical settings (60 images between 1 sec and 240 sec).

G. *in situ* assays of IKK activity

1. Stable Reconstitution of MEF IKK2$^{-/-}$

HA-IKK2 (N-terminal fusion) was cloned into pBABE-puro by previous lab members between EcoRI and SalI restriction sites, located between the 5' and 3' long terminal repeats. pBABE puro plasmid contained the DNA segment packaged into retrovirus for delivery into MEF cells. pCL-Eco encoded for the proteins that composed the viral package (Gag, pol, env). To generate virus 7 μg pBABE-puro and 3 μg pCL-Eco plasmids were mixed in 250 μL of DMEM (free of serum and PSG). After adding 30 μL of PEI and vortexing briefly, the mixture was incubated at room temperature for 15-30 min. This mixture was added dropwise to HEK 293T cells (seeded at 30% confluency the previous day) in a 6 cm TC dish with 3 mL of DMEM supplemented with 10% Fetal Bovine Serum and 1% Penicillin-Streptomycin-Glutamate (PSG). The next day, MEF IKK2$^{-/-}$ cells were seeded in 10 cm TC dish at 60-70% confluency in 10 mL of DMEM supplemented with Bovine Calf Serum and 1% PSG. On the third day, 36-42 hours post-transfection the supernatant of the HEK 293T was removed, filtered and added dropwise to MEF IKK2$^{-/-}$ TC dishes. Polybrene was added to the media for a final concentration of 4 μg/mL. TC dishes were gently agitated and then placed in 37ºC incubator for 2 days. On the 5th day, infected MEF IKK2$^{-/-}$ cells were split into 15 cm TC dishes (25 mL of media) and Puromycin was added to a final concentration of 5 μg/mL. Cells were kept in selection media until all MEF IKK2$^{-/-}$ control cells were dead (5-7 days).

2. MEF IKK2$^{-/-}$ m-TNF-α stimulation and lysis for western blot analysis

MEF IKK2$^{-/-}$ cells were seeded in 6 well TC plates at 80-95% confluency in 2 mL of media. 0.5 mg/mL of recombinant m-TNF-α was diluted to 10 μg/mL in DMEM and 2 μL of this

dilution was added to each 6 cm well. Cells were incubated with m-TNF-α for 10 minutes, media aspirated and then 1 mL of cold, sterile PBS was added to the cells.

Cells were lysed by scraping with cell scrapers, adding cells to Eppendorf centrifuge tubes, centrifugation, aspiration of PBS and then addition of cold RIPA buffer. Cells were resuspended in RIPA buffer (20 mM Tris pH 8, 200 mM NaCl, 1% Triton X-100, 5 mM 4-nitrophenyl phosphate di(Tris) Salt, 2 mM Sodium Orthovanadate, 1X Mammalian Protease Cocktail, 2 mM DTT) and then kept on ice for 30 min. After 30 minutes the Eppendorf tubes were centrifuged at 4ºC and the supernatant/lysate was collected. Bradford assay was utilized to determine the concentration of proteins.

3. Preparation of Nuclear Extract for Electromobility Shift Assay (EMSA)

Cells were passaged into 10 cm TC dishes at a confluency of 70-80%, depending on growth rate. The next day cells were treated with 10 ng/mL m-TNFα for 30 minutes. Media was aspirated and cells washed with cold DPBS. 1 mL of DPBS was added to TC dishes and the cells were scraped while on ice. Suspension was collected into 1.7 mL microcentrifuge tube and centrifuged for 5 min at 2000 rpm. Supernatant was aspirated, additional 1 mL cold PBS added for wash, centrifuged again and supernatant aspirated. Cell pellet was washed with 1 mL Buffer A (10mM HEPES pH 8.0, 1.5mM $MgCl_2$, 10mM KCl, 0.2mM DTT, 1mM PMSF, protease inhibitor; all of the latter three added fresh). Cells were lysed in 200 µL Buffer A (with additional 0.05% Triton X-100) for 10 minutes on ice. Lysates were then centrifuged 3000 rpm for 5 minutes at 4ºC. Supernatant (Cytosolic fraction) was aspirated. Pellet (Nucleosome) was washed with 1 mL Buffer A (no Triton X-100). After aspirating wash the pellet was resuspended in 50 µL Buffer C (20mM HEPES pH 8.0, 25% Glycerol, 0.42MNaCl, 1.5mM $MgCl_2$, 0.2mM EDTA, 0.2mM DTT, 1mM PMSF and protease inhibitor). Nuclear lysate was centrifuge at

13,200 rpm for 5 min at 4ºC. The supernatant (nuclear protein) was separated from the pellet and stored in a new microcentrifuge tube. A Bradford assay was performed, the nuclear lysate was flash frozen in liquid nitrogen and then stored at -80ºC.

III. Results

A. Purification of GST-NEMO Constructs in *E. coli* cells

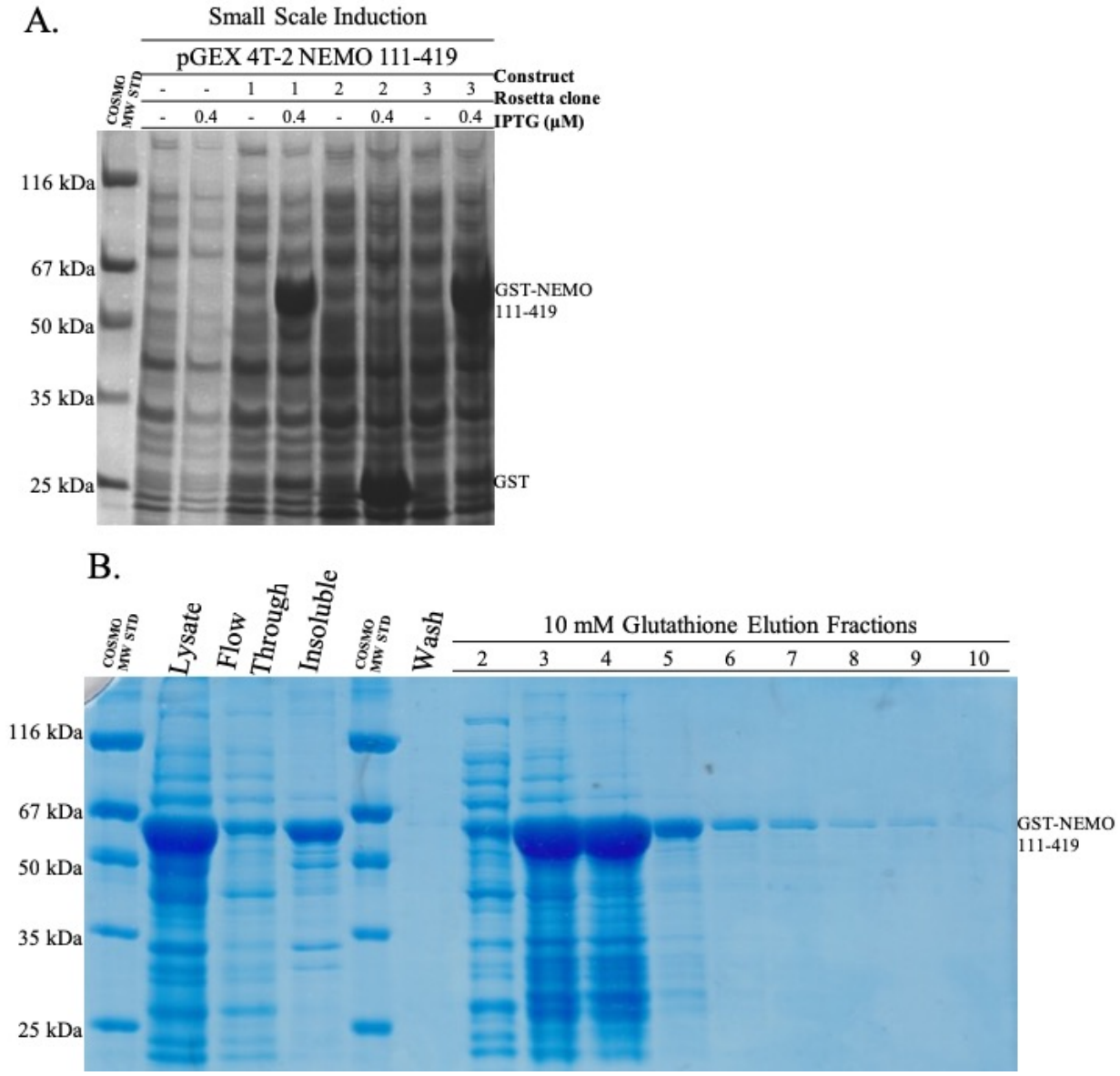

Figure 10. GST-NEMO 111-419 small scale expression and large scale purification.

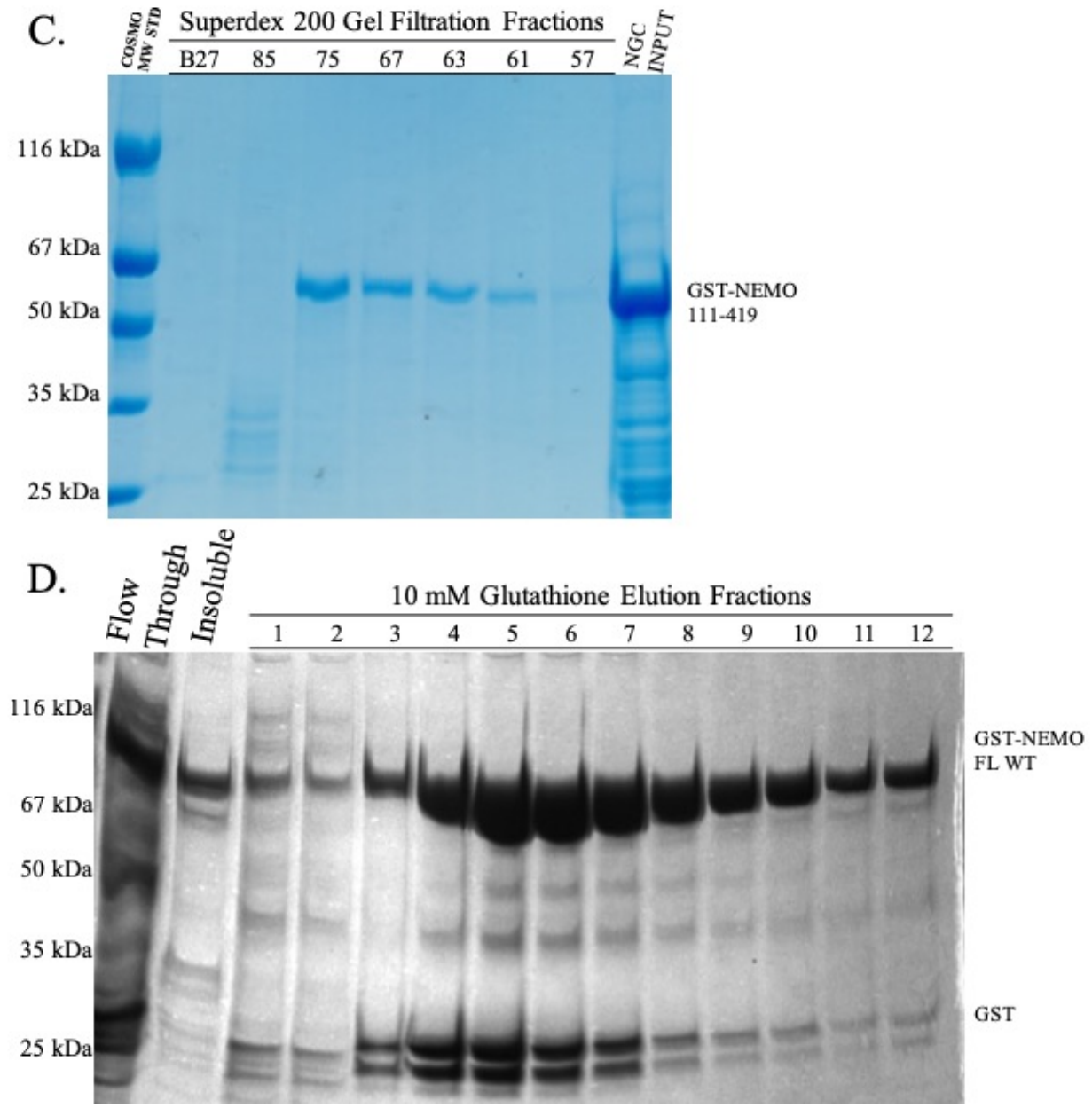

Figure 11. GST-NEMO 111-419 gel filtration and NEMO FL WT large scale purification

B. Purification of His_6-IKK2/β FL EE and AA from Sf9 cells

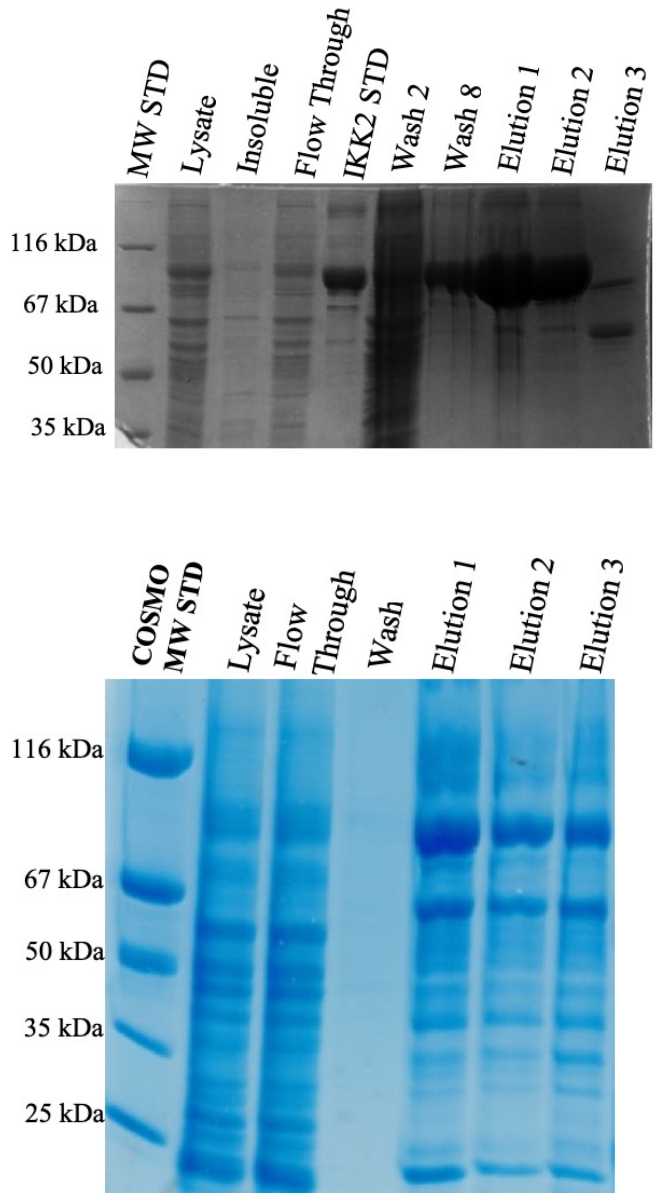

Figure 12. IKK2 FL EE and AA purification from Sf9 cells

C. Superose6 10/300 Resolution of NEMO-IKK2/β Complexes

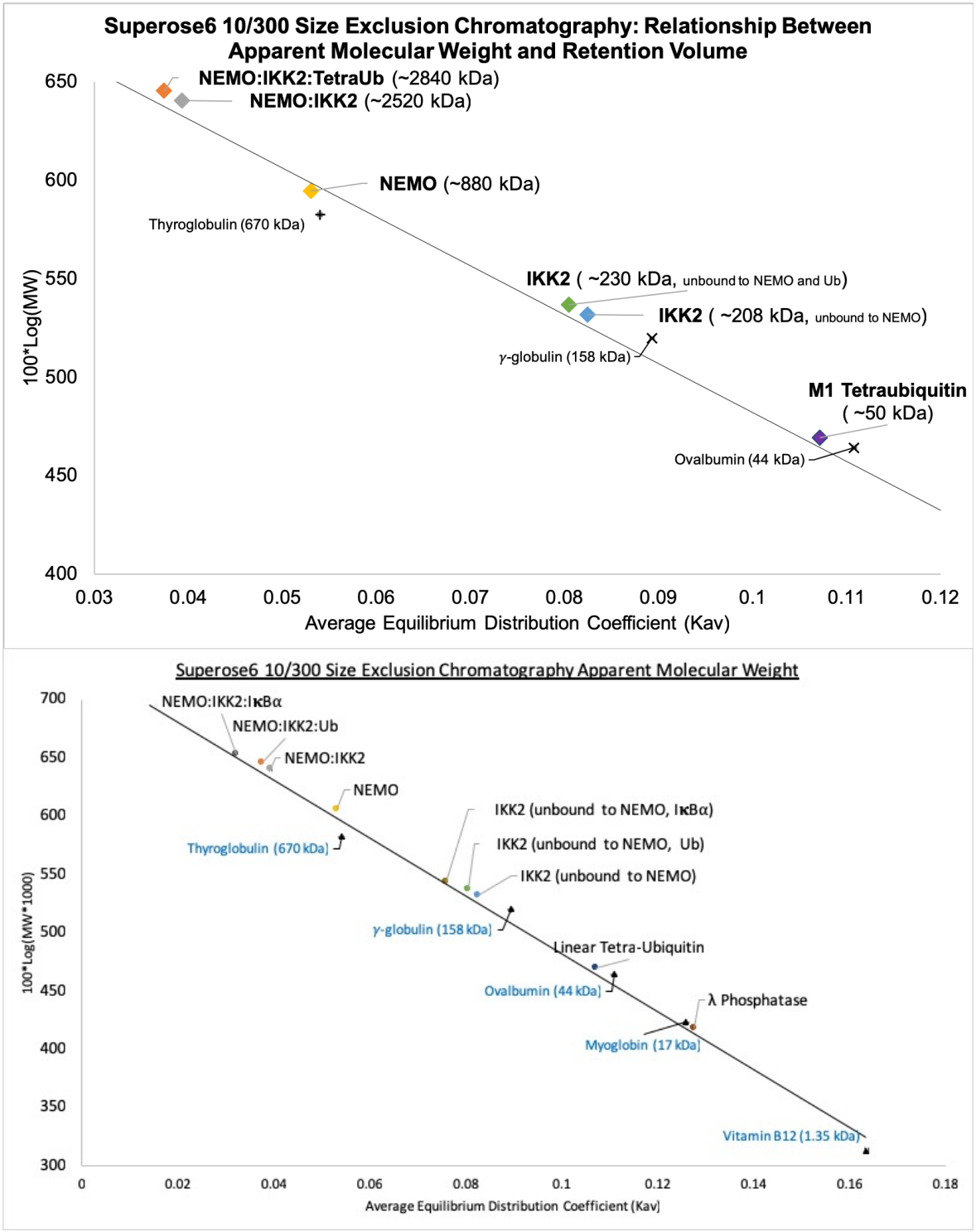

Figure 13. NEMO, IKK2 and linear Ub_4 chains (or IκBα) were resolved together or separately by gel filtration on Superose6 10/300 column (cross-linked agarose resin). NEMO:IKK2 complex in the presence of linear Ub_4 had a higher apparent molecular weight compared to NEMO:IKK2 complex without linear Ub_4.

Analysis of the IKK2:NEMO:Ub_4 complex by size exclusion chromatography.

Free NEMO, IKK2/β and Ub_4 were separately injected into a Superose6 10/30 size exclusion column fitted to BioRad NGC. Each protein eluted in mostly in a single peak. Equimolar amounts of NEMO, IKK2/β and Ub_4 were mixed and the mixture was injected into a Superose6 10/300 column fitted in BioRad NGC. The protein mixture was resolved into three peaks; corresponding to NEMO:IKK2/β, free IKK2/β and free Ub_4. This corresponded to a calculated apparent molecular weight of 2840 ± 30 kDa and 2520 ± 30 kDa respectively. Molecular weights were determined from a molecular weight standard. Moreover, blue dextran was essential for determining the void volume of the Superose6 10/300 column. Plotting the 100*log(MW*1000) against K_{av} yielded a relationship between the peak elution volume and molecular weight of the protein or protein complex.

As the proteins in the molecular weight standard are globular in shape, we cannot accurate determine the actual molecular weight of the NEMO protein in solution as NEMO is an elongated coiled coil structure. NEMO may be interacting with itself and the column. These interactions resulted in the large (880 ± 10 kDa) apparent molecular weight for NEMO FL treated with λ phosphatase. The MW of IKK2/β FL EE (unbound or free) gave a value of 205 ± 3 kDa. Free Ub_4 is ~ 40 kDa in size and the value is very similar to experimental value of ~50 kDa.

The NEMO:IKK2/β complex with or without also eluted at a high MW value and the peak of NEMO:IKK2/β:Ub_4 ternary binary complex shifted slightly relative to the NEMO:IKK2/β binary complex. The complex was treated with lambda phosphatase to remove any cryptic phosphorylation of IKK2/β that might be inhibitory to NEMO binding. The apparent MW of the ternary and binary complexes found to be 2840 ± 30 kDa and 2520 ± 30 kDa, respectively. However, it is unclear if this apparent high MW assembly is true or the complex

elutes abnormally due to abnormal migration of NEMO through the column matrix. However, if the complex is real high MW, we can estimate the number of NEMO units bound to IKK2/β dimers in the peak of the NEMO:IKK2/β complex. 7 IKK2/β dimers and 6 Ub_4 units were estimated to be bound to 6 NEMO FL dimers in the complex peak. SDS-PAGE analysis of the ternary complexes showed clear bands corresponding to IKK2/b and NEMO. But the Ub_4 band was not visible, although the ternary complex showed clear shifts in terms elution time. It is possible Ub_4 binds weakly and thus not be seen in the peak or it is bound sub-stoichiomerically which precludes its visualization due to low amount of protein loading.

The actual size of the IKK2/β, NEMO and Ub_4 complex cannot be accurately determined by SEC analysis. NEMO interaction with itself and the column causes a super shift in apparent molecular weight. Moreover, even though the number of IKK2/β dimers bound to NEMO can be calculated from the difference in apparent molecular weight (and this can be used to estimate the number of NEMO units present in the high molecular weight complex) there may be more NEMO interactions with the column which are enhanced or changed by the presence of other proteins.

A.

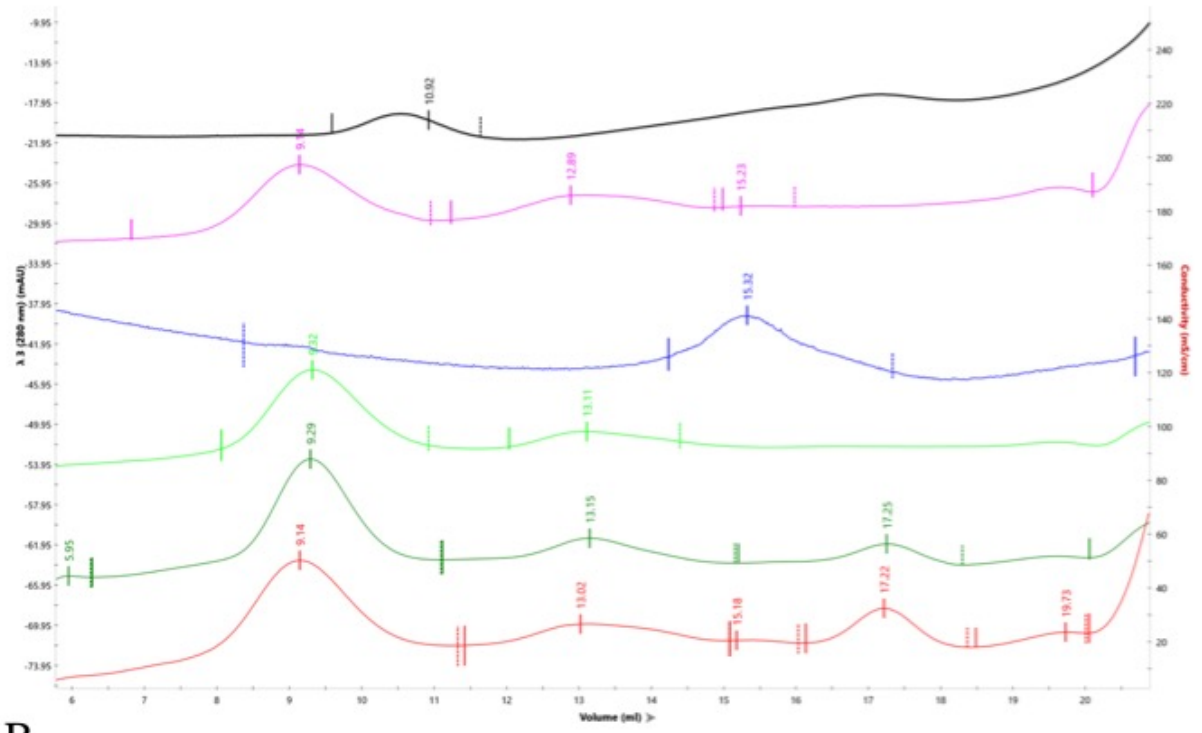

B.

Apparent Molecular Weight of Proteins and Protein Complexes

Protein Mixture Injected Into Column	NEMO:IKK2/β	NEMO	IKK2/β (free, unbound)	Ub_4	λpp
NEMO : λ Phosphatase		880 ± 10			17.0 ± 0.4
NEMO : IKK2/β FL EE : Ub_4	2840 ± 30		243 ± 4	53 ± 1	
Ub_4				50 ± 1	
NEMO : IKK2/β FL EE	2520 ± 30		211 ± 3		
NEMO : IKK2/β FL EE : λ Phosphatase	2570 ± 30		205 ± 3		14.0 ± 0.3
NEMO : IKK2/β FL EE : Ub_4: λ Phosphatase	2840 ± 30		224 ± 4	54 ± 1	14.3 ± 0.3

Figure 14. Apparent Molecular Weight of NEMO-IKK2/β Complexes Determined by Size Exclusion Chromatography.

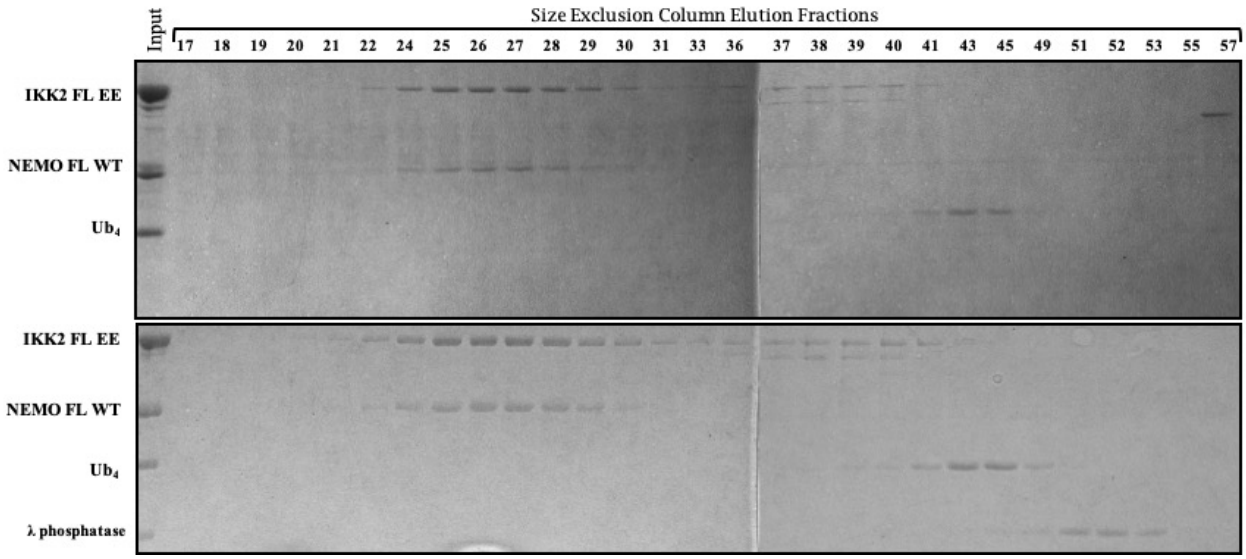

Figure 15. NEMO FL WT, IKK2/β FL EE and linear Ub_4 size exclusion chromatography (with or without λ phosphatase treatment). Approximately 27 µL of each elution fraction loaded in SDS acrylamide gels for SDS-PAGE. Electrophoresed gels were stained with Coomassie Brilliant Blue G-250.

D. GST Pulldown Assays

GST Pulldown Assays Reveals Transient Binding Interaction Between IKK2/β and NEMO

Since the discovery of NEMO and IKK2/β it has been known that the two proteins interaction strongly through Kinase Binding Domain (KBD) and NEMO Binding Domain (NBD) respectively. This interaction has a K_d of ~3-25 nM. I wished to investigate if NEMO and IKK2/β devoid of their primary binding interaction sites, KBD and NBD, can mediate binding to each other. To this end, I prepared four different versions of NEMO all fused with glutathione-S-transferase (GST) for the pull-down assay. Two different versions of IKK2/β were prepared- full length IKK2/β with C99A mutation and IKK2/β (11-669). The later construct was used for the structural studies. The C99A mutation does not affect catalytic activity of IKK2/β (unpublished results), although the protein used was prepared at least four years ago. Pull-down experiments were done in the presence or absence of a Met1 Ub-chain where four Ub moieties were fused linearly (Ub_4). However, GST-NEMO constructs lacking the KBD (residues 1-110) can pulldown recombinant IKK2/β FL C99A, and IKK2/β 11-669 EE (Figure 17, Figure 18). The immunoblot in figure 17, lanes 3-4, shows that IKK2/β binding at the transient binding domain in NEMO is weaker than binding mediated through KBD/NBD.

The lack of IKK2/β 11-669 EE pulldown by GST-NEMO FL (Figure 17) reveals that the N-terminus of NEMO may inhibit IKK2/β 11-669 binding. However, the molar concentrations of the proteins was very high relative to the volumes of beads, shown by the flow through in figure 4B lanes 5-6 (*which contained the same molar concentration of proteins as in figure 19*). As a result the majority of IKK2/β and GST-NEMO constructs were likely to have remained in the binding buffer after Glutathione resin was centrifuged/separated from flow through.

Nevertheless, my results clearly indicate NEMO and IKK2/β interact even when their high affinity binding sites are deleted. Moreover, interactions are significantly enhanced in the presence of Ub_4. The Ub_4-dependent binding enhancement is most visible when FL IKK2/β and C-terminal CC-LZ region of NEMO were used.

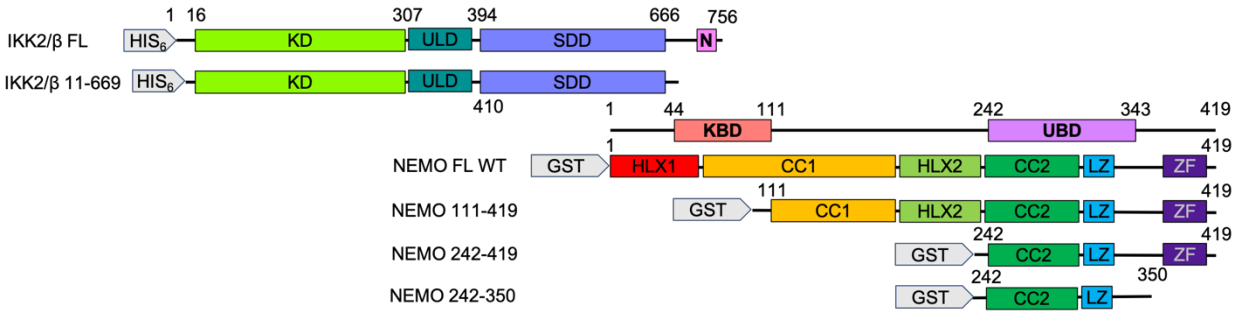

Figure 16. Domain Architecture of Protein Constructs. A schematic showing all GST-NEMO and IKK2/β constructs used in pulldown assays.

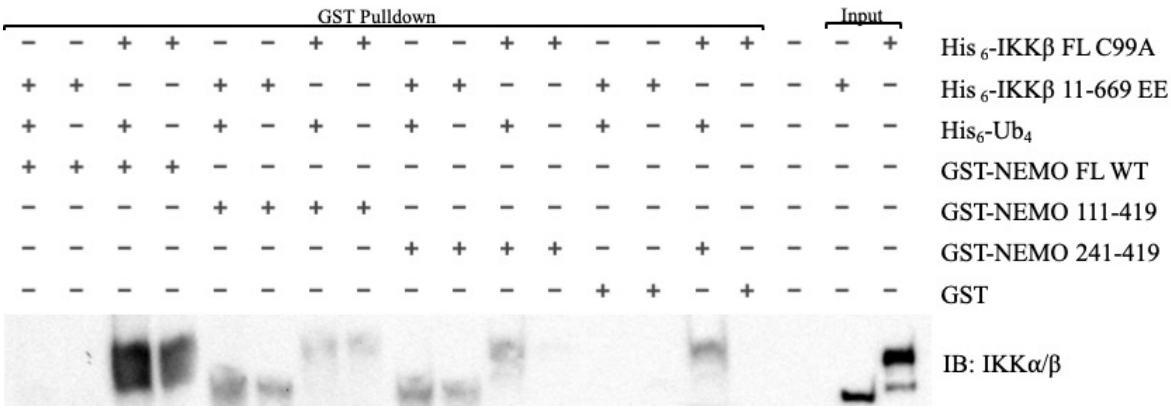

Figure 17. GST Pulldown Assay Reveals Potential Role of N-terminal IKK2/β in Binding to Ub_4 and/or NEMO. His-tagged IKKβ FL C99A was stored as glycerol stock at -20°C for minimum of four years. His-tagged IKKβ 11-669 EE was relatively fresh.

The C-terminal region beyond the CC-LZ domain is critical for the second site interaction between NEMO and IKK2/β.

Pulldown experiments were repeated using FL WT IKK2/β against four different GST-NEMO fusion proteins- 111-419, 241-419 and 241-350 (Figure 16). The highest quantity of IKK2/β FL SS (WT) had eluted with GST-NEMO 111-419 and 241-419 (Figure 18, lane 1 and 3) relative to the quantity of pulldown by GST NEMO 241-350 or GST control. IKK2/β FL SS pulldown was also enhanced in the presence of His_6-Ub_4 (Figure 18, lane 1 and 3). These results suggest that IKK2/β C99A and FL WT IKK2/β behave similarly in binding interactions. The most surprising result, however, is that the C-terminal Zn-finger domain is also critical in IKK2/β binding. Ubiquitin binding region of NEMO encompasses resides ~260-350. This region was crystallized with linear di-Ubiquitin [21]. Our results indicate that the region 350-419 of NEMO may be where transient binding to IKK2/β occurs. This region is the zinc finger of NEMO, which has been crystallized with K63 linked di-Ubiquitin. Alternatively, Ub_4 binds more strongly to NEMO (241-419) than NEMO (241-350) which indirectly favors IKK2/β binding. It is also possible that the NEMO (241-419):Ub_4 complex directly binds to IKK2/β.

Pulldown assays in Figure 19 also show that even NEMO FL WT and IKK2 FL C99A co-elution is enhanced by the addition of Ub_4 in the reaction mixture. Relative quantities of IKK2/β eluted in Lanes 5, 7, 9 and 11 (Figure 19) have a higher band intensity compared to the band intensities of reaction mixtures with the corresponding protein concentrations but lacking Ub_4 (lanes 6, 8, 10 and 12).

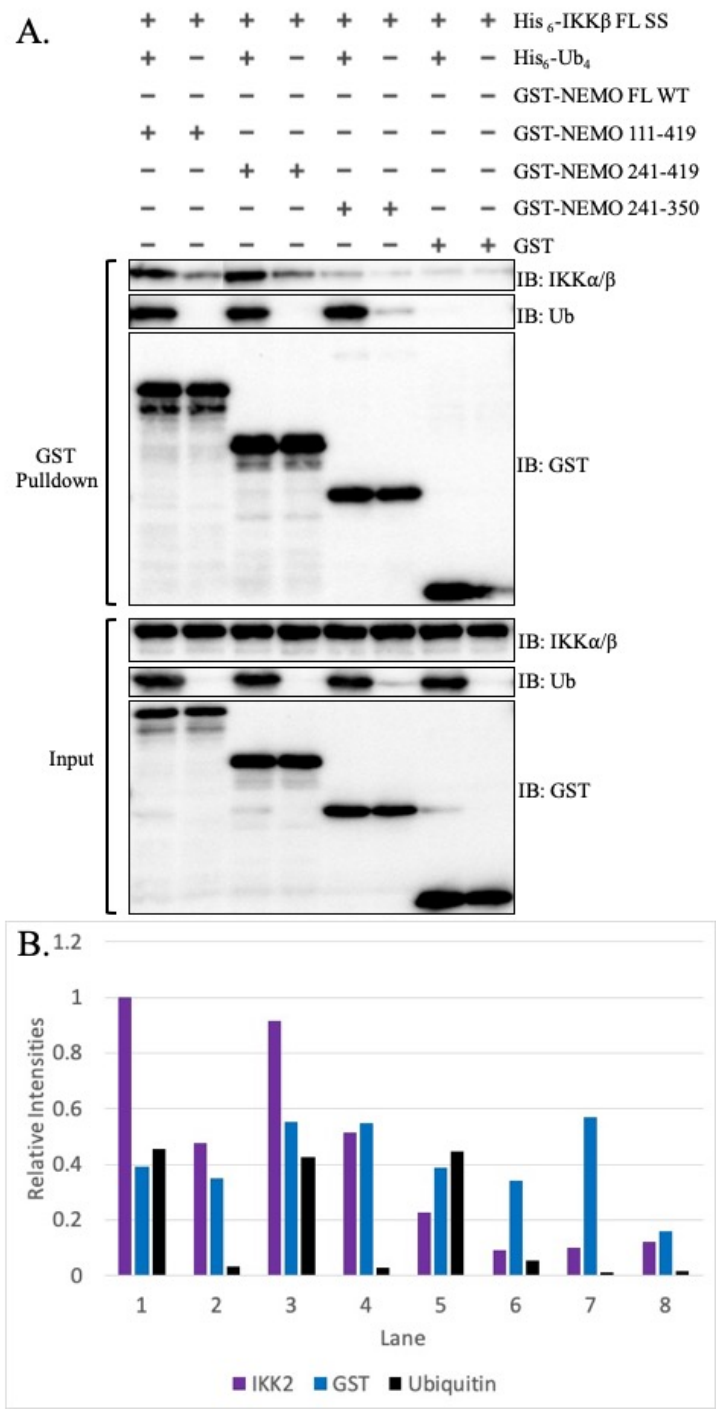

Figure 18. GST pulldown of IKK2/β FL SS. (A) Western Blot on PVDF membrane depicting results of GST-NEMO pulldowns with IKK2 FL SS and linear tetraubiquitin. The PD (pulldown) membrane immunoblotted with IKK1/2 antibody was the result of 28 µL of elution sample. The PD membrane immunoblotted with Ub or GST antibody was the result of 2µL of elution sample. (B) Relative band intensity compared to the IKK2 intensity in the first lane (immunoblots exposed at the same time point). The Ub immunoblot was developed after stripping the GST immunoblotted membrane, 3% BSA blocking and primary α-Ub incubation overnight.

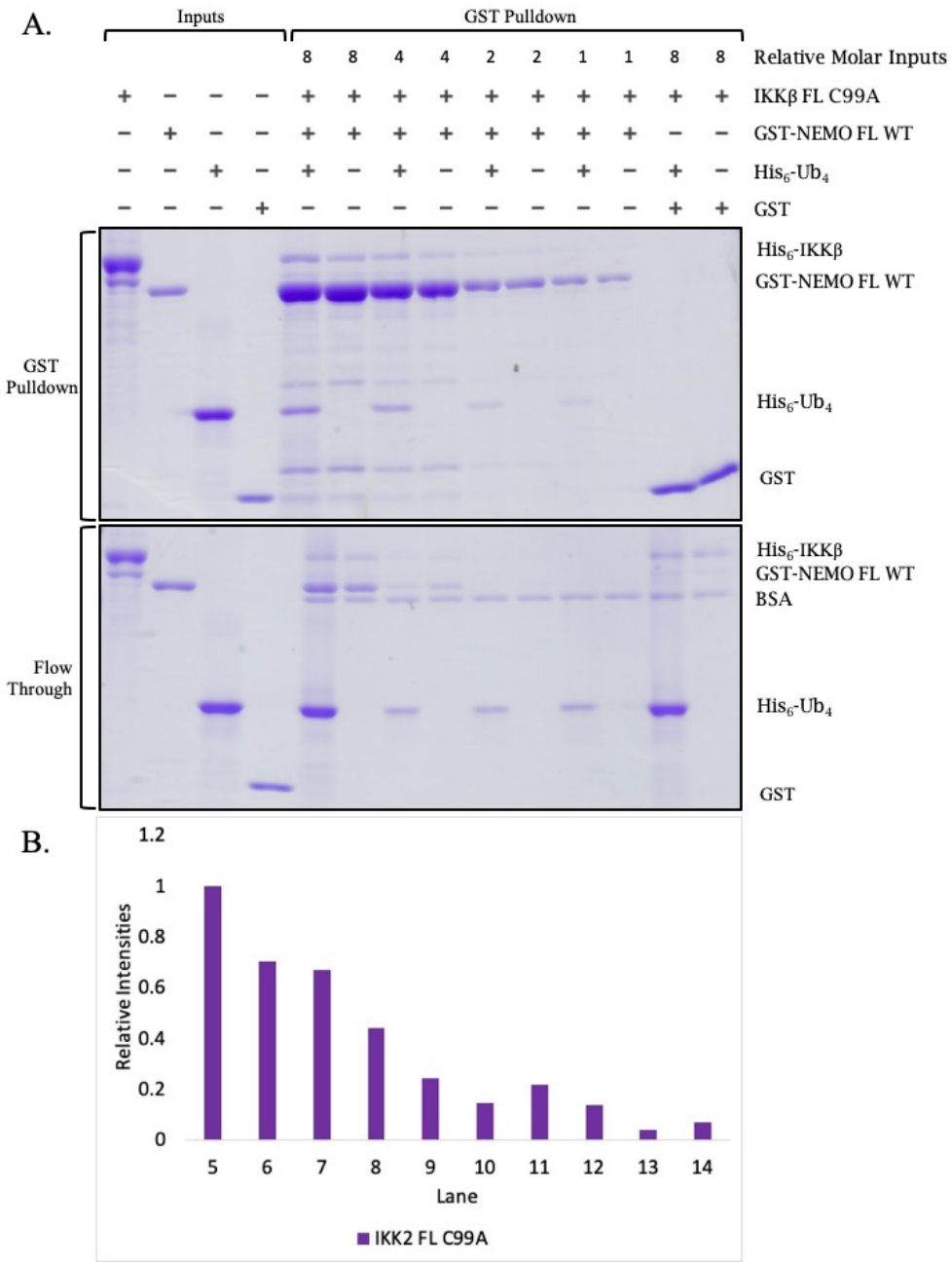

Figure 19. Linear Ub_4 enhances pulldown of IKK2/β FL C99A by GST-NEMO FL WT. (A) GST pulldowns with identical molar ratios of IKK2/β FL C99A, GST-NEMO FL WT and Linear Ub_4 were analyzed by Coomassie Brilliant Blue R-250. 6 µL of elution samples and flow throughs were separated by SDS-PAGE on their respective acrylamide gels. (B) All the IKK2/β band intensities were compared relative to the IKK2/β band in lane 5. (C) The intensities of bands corresponding to GST-NEMO FL WT, GST and Linear Ub_4 were also scaled relative to the intensity of the IKK2/β Coomassie signal in lane 5.

E. MEF IKK2$^{-/-}$ Reconstitution and Measurements of Kinase Activity

Reconstitution of WT and IKK2/β mutants in IKK2/β$^{-/-}$ MEFs

IKK2/β$^{-/-}$ MEF cell lines are useful models for determining the effects of IKK2/β mutations on catalytic activity by reconstituting WT or mutants in these IKK-deficient cell lines. IKK2/β activity can be measured in several different ways – monitoring the IKK2/β activation loop phosphorylation using a phosphor-Ser181-specific antibody, measuring catalytic activity in vitro from immunoprecipitated IKK2/β, measuring the levels of IκBα by WB, and measuring DNA binding activity of nuclear NF-kB using EMSA. I wanted to test several mutants (I413A, L414A, K418, etc) previously generated in our lab as well as test some new mutant stable cell lines (Y169A, Y169E, Y169R, E522A, Q523A, R526A, E527A) that I made.

The retrovirus delivering the HA- IKK2/β constructs to rescue the IKK2/β$^{-/-}$ is based upon the Moloney Murine Leukemia Virus [36]. HA-IKK2/β cloned in between the 5' and 3' long terminal repeats was incorporated into the chromosomal DNA of the infected IKK2/β$^{-/-}$ cell. The viral promoter upstream of the gene is responsible for HA-IKK2/β expression. To analyze the effects of mutations on IKK activation or its catalytic activity in the reconstituted stable cell lines, IKK2/β expression levels need to be determined by Western blot (WB). The level of expression needs to be identical for the different IKK2/β cell lines to be better comparison of activity between wt and mutants. Although I tested the expression of wt and mutant IKK2/β (Fig 20), my confidence diminished when I repeated the experiment and found that the antibody might be recognizing a non-specific band (Fig. 21).

I am now confident about the expression of WT IKK2/β in reconstituted cells since both HA and IKK2/β-specific antibodies identified the IKK2/β band that is not present in the KO cells. In the future I will test the expression of the mutants and their activities as described above.

Some of these mutants however were tested previously in the lab and L413A and I414A mutants were found to be defective in IKK2/β activation. A transfection-based experiments also revealed similar results.

I have prepared the nuclear extracts from the KO and WT IKK2/β-reconstituted cells that had stable transfection. EMSA assay showed that WT IKK2/β reconstituted cells had nuclear NF-κB while the KO did not.

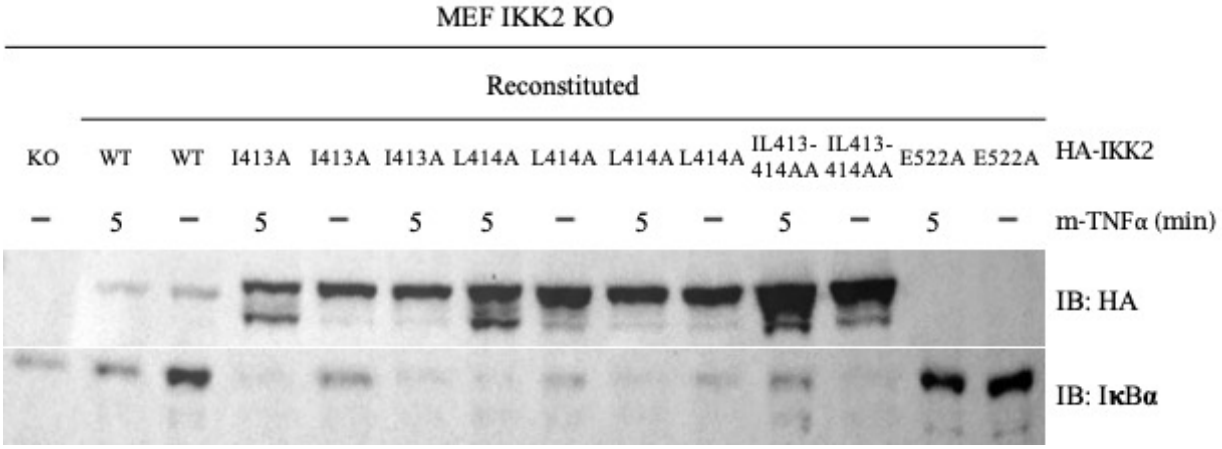

Figure 20. MEF IKK2 KO Stable Reconstitution and Western Blot Optimization. MEF IKK2 KO polyclonal cell lines were transduced by retroviruses containing HA-IKK2 constructs (mouse). MEF IKK2 KO cell lines were treated with m-TNFα, lysed and analyzed by western blot. Western blots revealed the expression of HA-IKK2 and potential effect that mutations had on IκBα degradation. Mutant residues were selected based upon their location in the potential transient binding region in IKK2.

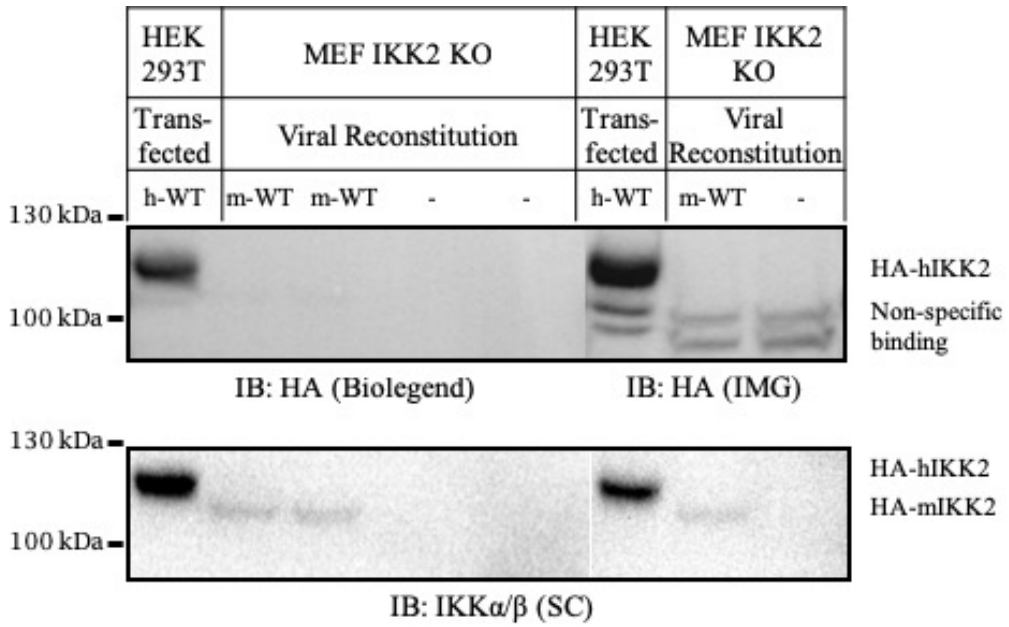

Figure 21. MEF IKK2 KO Cell Line IKK2 Western Blot Optimization and Proper Positive Controls. MEF IKK2 KO, WT reconstituted cells and HA-IKK2 (human) transfected HEK 293T lysates were separated by SDS-PAGE and transferred to PVDF membrane. PVDF membranes previously immunoblotted with HA antibodies were stripped and immunoblotted with IKKα/β antibody.

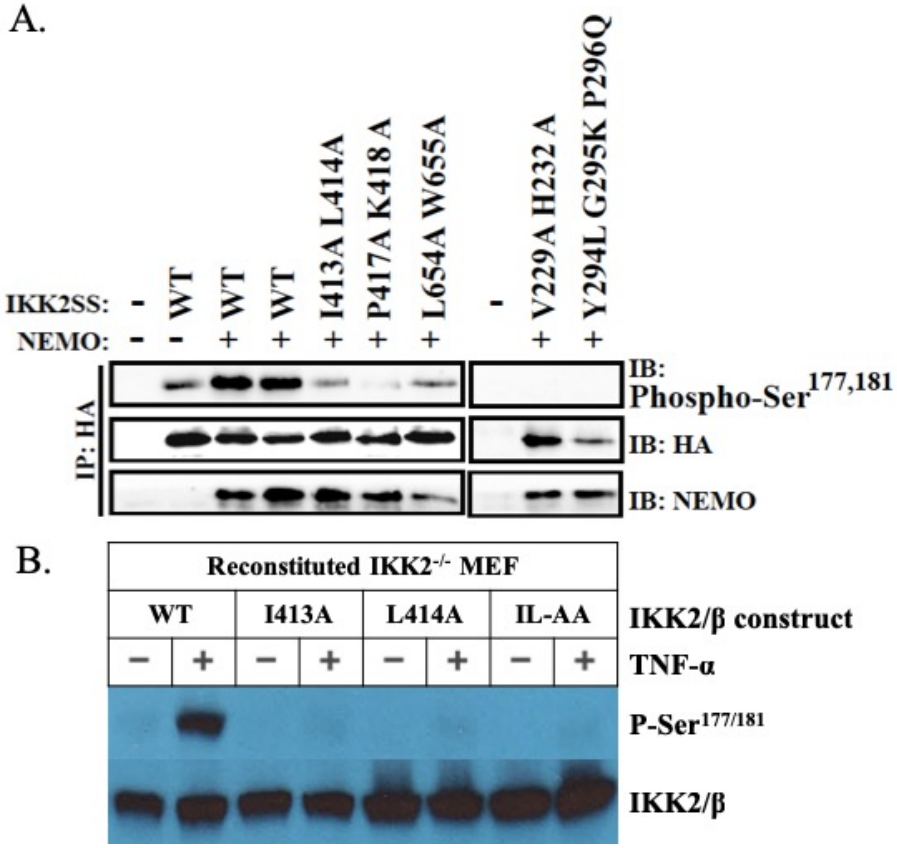

Figure 22. Previous Results Showing Effect of V-surface Mutations in IKK2 [31].

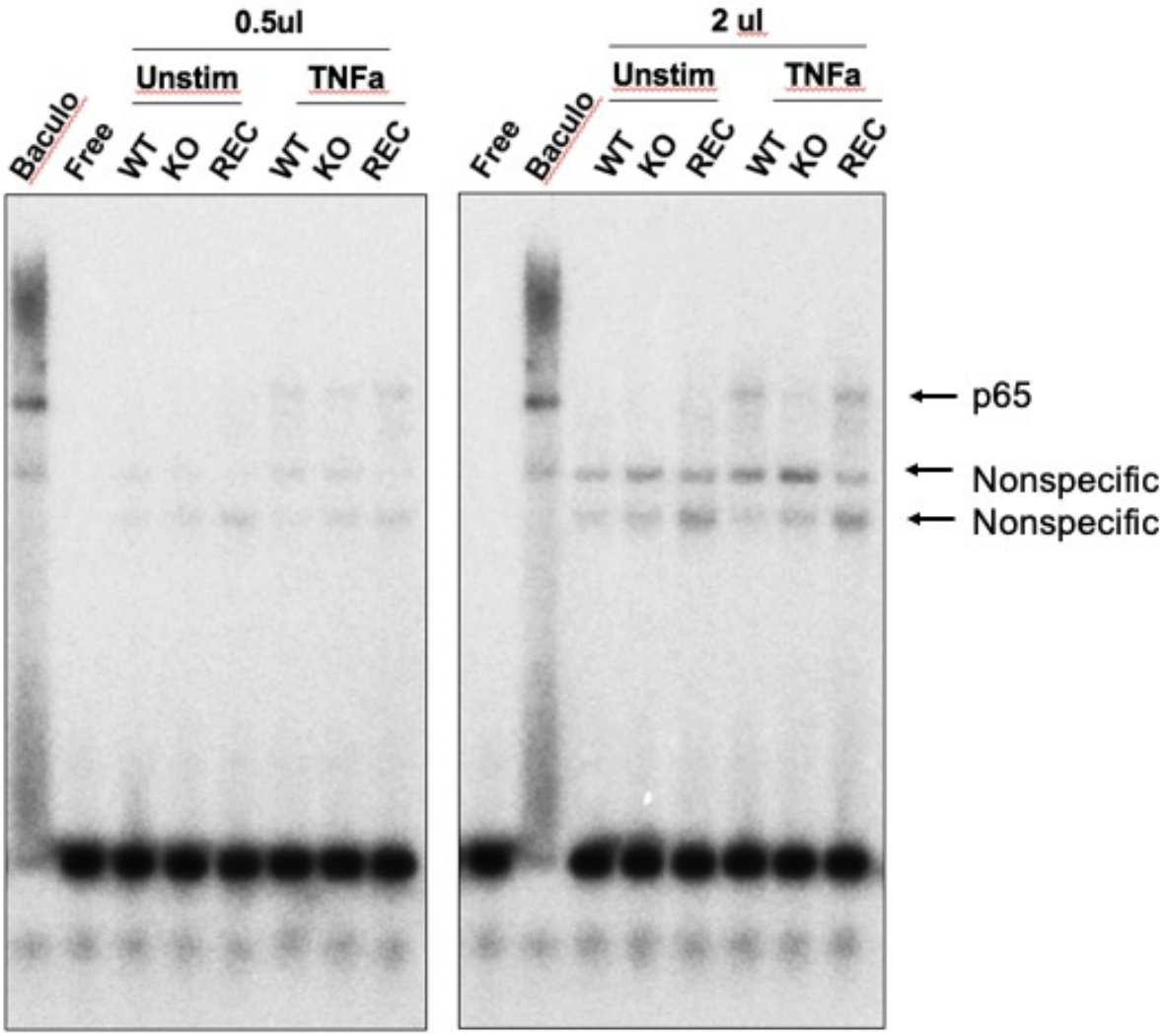

Figure 23. EMSA of MEF$^{IKK2-/-}$ Cell Line Nuclear Lysates with E-selectin Probe. Nuclear translocation of NF-κB or p65 was measured by analyzing the relative quantity of binding to radioactively labeled E-selectin. MEF$^{IKK2-/-}$, MEF$^{IKK2-/-\ rec\ WT}$ or MEF^{WT} cells were untreated or treated with m-TNF-α (recombinant) for 30 minutes before fractionating cytosolic extract and nuclear extract.

IV. Discussion

A. *In vitro* Interaction Between IKK2/β, NEMO and Ub_4

Determining the mechanism of IKK activation requires an understanding of the proteins participating. IKK2/β and NEMO are already well known essential proteins in NF-κB activation. M1 linked Ub_n chains are also established as essential in activation. Upon stimuli induced IKK activation, M1 Ub_n chains are generated *in situ*, indicating a role in activation [19, 21, 24]. Moreover, *in vitro* assays have previously shown that addition of M1 Ub_n chains is sufficient for IKK activation [25, 26]. However, it is unknown *how* exactly M1 Ub_n chains participate in activation. To this end, I had set out to establish how these three proteins behave *in vitro* by size exclusion chromatography.

The large (880 ± 10 kDa) apparent molecular weight for NEMO FL treated with λ phosphatase is actually a 113 kDa NEMO dimer as determined by SEC-MALS using Superose6 10/300 for gel filtration [22]. This indicates that NEMO migrates abnormal through the column matrix.

Since IKK2/β 11-669 structure has been determined to be a dimer by crystal structures [31] we can assume that the apparent molecular weight represents an IKK2/β FL EE dimer. Moreover, 205 kDa apparent MW is similar in size to the 178 kDa theoretical MW of the IKK2/β dimer. Previous literature has shown an apparent molecular weight of 240 ± 10 kDa for IKK2/β dimer and a 200 kDa MW for cross-linked IKK2/β [8]. Free Ub_4 is ~ 40 kDa in size and the value is very similar to experimental value of ~50 kDa. The molecular weight as determined by SEC-MALS was determined to be 186 kDa [22]. All these values confirm that the peak observed correlated with IKK2/β dimer.

The apparent MW of the ternary and binary complexes found to be 2840 ± 30 kDa and 2520 ± 30 kDa, respectively. 7 IKK2/β dimers and 6 Ub_4 units were estimated to be bound to 6

NEMO FL dimers in the complex peak. This is contrast to SEC-MALS data suggesting that the NEMO-IKK2/β is ~2000 kDa in size with 12-16 dimers [22] in approximately stoichiometric quantities. Our results support the model that NEMO-IKK2/β forms higher-order oligomers form together in size exclusion chromatography.

SDS-PAGE analysis of the ternary complexes showed clear bands corresponding to IKK2/β and NEMO. But the Ub_4 band was not visible, although the ternary complex showed clear shifts in terms elution time. It is possible Ub_4 binds weakly and thus not be seen in the peak or it is bound sub-stoichiometrically which precludes its visualization due to low amount of protein loading.

Eventually future experiments can be conducted to determine the effect that linear Ub_4 has on the formation of ternary complex, NEMO-IKK2/β binding through the second site interaction or higher order oligomerization. To do this, SEC-MALS analysis of NEMO-Ub_4 fusion protein and IKK2/β may reveal the effects of Ub_4 conjugation. Fusion NEMO-Ub_4 will force stoichiometric quantities of Ub_4 within the complex.

B. M1 Ub_4 Enhances IKK2/β-NEMO binding in secondary site of interaction

Since the discovery of NEMO and IKK2/β it has been known that the two proteins interaction strongly through Kinase Binding Domain (KBD) and NEMO Binding Domain (NBD) respectively. This interaction has a K_d of ~3-25 nM [24, 43]. However, GST-NEMO constructs lacking the KBD (residues 1-110) can pulldown recombinant IKK2/β FL C99A, and IKK2/β 11-669 EE.

The lack of IKK2/β 11-669 EE pulldown by GST-NEMO FL in reveals that the N-terminus of NEMO may inhibit IKK2/β 11-669 binding. However, the molar concentrations of the proteins was very high relative to the volumes of beads, shown by the flow through (*which contained the same molar concentration of proteins as the third pulldown assay*). As a result the majority of IKK2/β and GST-NEMO constructs were likely to have remained in the binding buffer after Glutathione resin was centrifuged/separated from flow through. Nevertheless, my results clearly indicate NEMO and IKK2/β interact even when their high affinity binding sites are deleted. Moreover, interactions are significantly enhanced in the presence of Ub_4. The Ub_4-dependent binding enhancement is most visible when FL IKK2/β and C-terminal CC-LZ region of NEMO were used.

M1 Ub_n roles in IKK activation are being explored. This secondary site of interaction, enhanced by M1 Ub_n may be a key part of IKK activation. The secondary binding domain has been narrowed down to the C-terminal CC-LZ region in NEMO and the V-surface in IKK2/β as shown by previous lab members [31].

C. The C-terminal region beyond the CC-LZ domain is critical for the second site interaction between NEMO and IKK2/β.

The highest quantity of IKK2/β FL SS (WT) had eluted with GST-NEMO 111-419 and 241-419 (Figure 2, lane 1 and 3). Which conveys the novel result that the C-terminal Zn-finger domain is also critical in IKK2/β binding, in addition to the NBD-KBD 3-25 nM interaction. Ubiquitin binding region of NEMO encompasses resides ~260-350. This region was crystallized with linear di-Ubiquitin [21, 24]. Our results indicate that the region 350-419 of NEMO may be where transient binding to IKK2/β occurs. This region is the zinc finger of NEMO, which has been crystallized with K63 linked di-Ubiquitin. Alternatively, Ub_4 binds more strongly to NEMO (241-419) than NEMO (241-350) which indirectly favors IKK2/β binding. It is also possible that the NEMO (241-419):Ub_4 complex directly binds to IKK2/β.

Pulldown assays also show that even NEMO FL WT and IKK2 FL C99A co-elution is enhanced by the addition of Ub_4 in the reaction mixture. Relative quantities of IKK2/β eluted in lanes 5, 7, 9 and 11 have a higher band intensity compared to the band intensities of (lanes 6, 8, 10 and 12) which lack Ub_4 in the binding reaction.

It would be interesting to observe how mutant constructs of either NEMO CC-LZ or IKK2/β V-surface affect second site interaction.

D. Potential Role of Transient Binding Domain in IKK trans-autophosphorylation

Previously created mutants in the V-shape interface of IKK2/β and reconstituted in MEF IKK2$^{-/-}$ showed a decreased ability to trans-autophosphorylate [31]. Despite this inability to trans-autophosphorylate other IKK units, constitutively active IKK2/β mutants were still able to phosphorylate IκBα; meaning the mutants in the V-shape interface did not affect the kinase ability of IKK2/β. Initially the theory was that IKK2/β dependent oligomerization was responsible for trans-autophosphorylation [31]. However over-expressed IKK2/β did not form an oligomer in size exclusion chromatography. Rather IKK2/β had dimerized [31]. Yet, only in the presence of NEMO we observe a high molecular weight complex. Thus, oligomerization may be directly facilitated through NEMO or alternatively by IKK2/β adopting different conformations upon NEMO binding. Moreover, the presence of Ub_4 may play a role in this NEMO dependent oligomerization of IKK which leads to activation.

A recently published paper had shown that B14, a vaccinia viral protein, binds to IKK2/β around the transient binding region which directly prevent IKK2/β trans-autophosphorylation [14]. This may support the role that the transient binding region of IKK2/β plays in trans-autophosphorylation.

Single amino acid substitutions in the transient binding site of IKK2/β may have prevented the observed transient binding with NEMO and this may be correlated with the observed decreased in trans-autophosphorylation of IKK2/β.

Whether NEMO and Ub_4 play a pivotal role in direct or indirect IKK2/β oligomerization/activation will have to be explored. My results may indicate that IKK mutants which are defective in trans-autophosphorylation potentially lack Ub_4 dependent NEMO 339-419 interaction in the IKK2/β V-surface.

REFERENCES

[1] Karin, M., and Y. Ben-Neriah. “Phosphorylation Meets Ubiquitination: The Control of NF-[Kappa]B Activity.” *Annual Review of Immunology* 18 (2000): 621–63.

[2] Solt, Laura A., and Michael J. May. “The IkappaB Kinase Complex: Master Regulator of NF-KappaB Signaling.” *Immunologic Research* 42, no. 1–3 (2008): 3–18.

[3] Scheidereit, Claus. “IkappaB Kinase Complexes: Gateways to NF-KappaB Activation and Transcription.” *Oncogene* 25, no. 51 (October 30, 2006): 6685–6705.

[4] Li, Z. W., W. Chu, Y. Hu, M. Delhase, T. Deerinck, M. Ellisman, R. Johnson, and M. Karin. “The IKKbeta Subunit of IkappaB Kinase (IKK) Is Essential for Nuclear Factor KappaB Activation and Prevention of Apoptosis.” *The Journal of Experimental Medicine* 189, no. 11 (June 7, 1999): 1839–45.

[5] Delhase, M., M. Hayakawa, Y. Chen, and M. Karin. “Positive and Negative Regulation of IkappaB Kinase Activity through IKKbeta Subunit Phosphorylation.” *Science (New York, N.Y.)* 284, no. 5412 (April 9, 1999): 309–13.

[6] Mercurio, F., Zhu, H., Murray, B.W., Shevchenko, A., Bennett, B.L., Li, J., Young, D.B., Barbosa, M., Mann, M., Manning, A., Rao, A., 1997. IKK-1 and IKK-2: cytokine-activated IkappaB kinases essential for NF-kappaB activation. Science 278, 860–866.

[7] Li, Q., D. Van Antwerp, F. Mercurio, K. F. Lee, and I. M. Verma. “Severe Liver Degeneration in Mice Lacking the IkappaB Kinase 2 Gene.” *Science (New York, N.Y.)* 284, no. 5412 (April 9, 1999): 321–25.

[8] Zandi, E., Y. Chen, and M. Karin. “Direct Phosphorylation of IkappaB by IKKalpha and IKKbeta: Discrimination between Free and NF-KappaB-Bound Substrate.” *Science (New York, N.Y.)* 281, no. 5381 (August 28, 1998): 1360–63.

[9] Li, X. H., X. Fang, and R. B. Gaynor. “Role of IKKgamma/Nemo in Assembly of the Ikappa B Kinase Complex.” *The Journal of Biological Chemistry* 276, no. 6 (February 9, 2001): 4494–4500.

[10] Rothwarf, D. M., E. Zandi, G. Natoli, and M. Karin. “IKK-Gamma Is an Essential Regulatory Subunit of the IkappaB Kinase Complex.” *Nature* 395, no. 6699 (September 17, 1998): 297–300.

[11] Courtois, Gilles, and Marie-Odile Fauvarque. “The Many Roles of Ubiquitin in NF-KB Signaling.” *Biomedicines* 6, no. 2 (April 10, 2018).

[12] Skaug, Brian, Xiaomo Jiang, and Zhijian J. Chen. “The Role of Ubiquitin in NF-KappaB Regulatory Pathways.” *Annual Review of Biochemistry* 78 (2009): 769–96.

[13] Ashida, Hiroshi, Minsoo Kim, Marc Schmidt-Supprian, Averil Ma, Michinaga Ogawa, and Chihiro Sasakawa. “A Bacterial E3 Ubiquitin Ligase IpaH9.8 Targets

NEMO/IKKgamma to Dampen the Host NF-KappaB-Mediated Inflammatory Response." *Nature Cell Biology* 12, no. 1 (January 2010): 66–73; sup pp 1-9.

[14] Tang, Qingyu, Sayan Chakraborty, and Guozhou Xu. "Mechanism of Vaccinia Viral Protein B14-Mediated Inhibition of IκB Kinase β Activation." *The Journal of Biological Chemistry* 293, no. 26 (June 29, 2018): 10344–52.

[15] Baker, Rebecca G., Matthew S. Hayden, and Sankar Ghosh. "NF-KB, Inflammation, and Metabolic Disease." *Cell Metabolism* 13, no. 1 (January 5, 2011): 11–22.

[16] Abbott, Derek W., Andrew Wilkins, John M. Asara, and Lewis C. Cantley. "The Crohn's Disease Protein, NOD2, Requires RIP2 in Order to Induce Ubiquitinylation of a Novel Site on NEMO." *Current Biology: CB* 14, no. 24 (December 29, 2004): 2217–27.

[17] Maubach, Gunter, Ann-Christin Schmädicke, and Michael Naumann. "NEMO Links Nuclear Factor-KB to Human Diseases." *Trends in Molecular Medicine* 23, no. 12 (2017): 1138–55.

[18] Wu, Chuan-Jin, Dietrich B. Conze, Tao Li, Srinivasa M. Srinivasula, and Jonathan D. Ashwell. "Sensing of Lys 63-Linked Polyubiquitination by NEMO Is a Key Event in NF-KappaB Activation [Corrected]." *Nature Cell Biology* 8, no. 4 (April 2006): 398–406.

[19] Hauenstein, Arthur V., W. Eric Rogers, Jacob D. Shaul, De-Bin Huang, Gourisankar Ghosh, and Tom Huxford. "Probing Kinase Activation and Substrate Specificity with an Engineered Monomeric IKK2." *Biochemistry* 53, no. 12 (April 1, 2014): 2064–73.

[20] Chen, Zhijian J. "Ubiquitination in Signaling to and Activation of IKK." *Immunological Reviews* 246, no. 1 (March 2012): 95–106.

[21] Lo, Yu-Chih, Su-Chang Lin, Carla C. Rospigliosi, Dietrich B. Conze, Chuan-Jin Wu, Jonathan D. Ashwell, David Eliezer, and Hao Wu. "Structural Basis for Recognition of Diubiquitins by NEMO." *Molecular Cell* 33, no. 5 (March 13, 2009): 602–15.

[22] Hauenstein, Arthur V., Guozhou Xu, Venkataraman Kabaleeswaran, and Hao Wu. "Evidence for M1-Linked Polyubiquitin-Mediated Conformational Change in NEMO." *Journal of Molecular Biology* 429, no. 24 (December 8, 2017): 3793–3800.

[23] Kensche, Tobias, Fuminori Tokunaga, Fumiyo Ikeda, Eiji Goto, Kazuhiro Iwai, and Ivan Dikic. "Analysis of Nuclear Factor-KB (NF-KB) Essential Modulator (NEMO) Binding to Linear and Lysine-Linked Ubiquitin Chains and Its Role in the Activation of NF-KB." *The Journal of Biological Chemistry* 287, no. 28 (July 6, 2012): 23626–34.

[24] Grubisha, O., Kaminska, M., Duquerroy, S., Fontan, E., Cordier, F., Haouz, A., Raynal, B., Chiaravalli, J., Delepierre, M., Israël, A., Véron, M., Agou, F., 2010. DARPin-assisted crystallography of the CC2-LZ domain of NEMO reveals a coupling between dimerization and ubiquitin binding. J. Mol. Biol. 395, 89–104.

[25] Xia, Zong-Ping, Lijun Sun, Xiang Chen, Gabriel Pineda, Xiaomo Jiang, Anirban Adhikari, Wenwen Zeng, and Zhijian J. Chen. "Direct Activation of Protein Kinases by Unanchored Polyubiquitin Chains." *Nature* 461, no. 7260 (September 3, 2009): 114–19.

[26] Tokunaga, F., Sakata, S., Saeki, Y., Satomi, Y., Kirisako, T., Kamei, K., Nakagawa, T., Kato, M., Murata, S., Yamaoka, S., Yamamoto, M., Akira, S., Takao, T., Tanaka, K., Iwai, K., 2009. Involvement of linear polyubiquitylation of NEMO in NF-kappaB activation. Nat. Cell Biol. 11, 123–132.

[27] Bal, E., Laplantine, E., Hamel, Y., Dubosclard, V., Boisson, B., Pescatore, A., Picard, C., Hadj-Rabia, S., Royer, G., Steffann, J., Bonnefont, J.-P., Ursini, V.M., Vabres, P., Munnich, A., Casanova, J.-L., Bodemer, C., Weil, R., Agou, F., Smahi, A., 2017. Lack of interaction between NEMO and SHARPIN impairs linear ubiquitination and NF-κB activation and leads to incontinentia pigmenti. J. Allergy Clin. Immunol. 140, 1671-1682.e2.

[28] Tarantino, Nadine, Jean-Yves Tinevez, Elizabeth Faris Crowell, Bertrand Boisson, Ricardo Henriques, Musa Mhlanga, Fabrice Agou, Alain Israël, and Emmanuel Laplantine. "TNF and IL-1 Exhibit Distinct Ubiquitin Requirements for Inducing NEMO-IKK Supramolecular Structures." *The Journal of Cell Biology* 204, no. 2 (January 20, 2014): 231–45.

[29] Xu, Guozhou, Yu-Chih Lo, Qiubai Li, Gennaro Napolitano, Xuefeng Wu, Xuliang Jiang, Michel Dreano, Michael Karin, and Hao Wu. "Crystal Structure of Inhibitor of KB Kinase β." *Nature* 472, no. 7343 (April 21, 2011): 325–30.

[30] Rushe, M., Silvian, L., Bixler, S., Chen, L.L., Cheung, A., Bowes, S., Cuervo, H., Berkowitz, S., Zheng, T., Guckian, K., Pellegrini, M., Lugovskoy, A., 2008. Structure of a NEMO/IKK-associating domain reveals architecture of the interaction site. Structure 16, 798–808.

[31] Polley, S., Huang, D.-B., Hauenstein, A.V., Fusco, A.J., Zhong, X., Vu, D., Schröfelbauer, B., Kim, Y., Hoffmann, A., Verma, I.M., Ghosh, G., Huxford, T., 2013. A structural basis for IκB kinase 2 activation via oligomerization-dependent trans auto-phosphorylation. PLoS Biol. 11, e1001581.

[32] Ivins, Frank J., Mark G. Montgomery, Susan J. M. Smith, Aylin C. Morris-Davies, Ian A. Taylor, and Katrin Rittinger. "NEMO Oligomerization and Its Ubiquitin-Binding Properties." *The Biochemical Journal* 421, no. 2 (June 26, 2009): 243–51.

[33] Tang, Eric D., Naohiro Inohara, Cun-Yu Wang, Gabriel Nuñez, and Kun-Liang Guan. "Roles for Homotypic Interactions and Transautophosphorylation in IkappaB Kinase Beta IKKbeta) Activation [Corrected]." *The Journal of Biological Chemistry* 278, no. 40 (October 3, 2003): 38566–70.

[34] Mulero, Maria Carmen, De-Bin Huang, H. Thien Nguyen, Vivien Ya-Fan Wang, Yidan Li, Tapan Biswas, and Gourisankar Ghosh. "DNA-Binding Affinity and Transcriptional Activity of the RelA Homodimer of Nuclear Factor KB Are Not Correlated." *The Journal of Biological Chemistry* 292, no. 46 (17 2017): 18821–30.

[35] Mulero, Maria Carmen, Shandy Shahabi, Myung Soo Ko, Jamie M. Schiffer, De-Bin Huang, Vivien Ya-Fan Wang, Rommie E. Amaro, Tom Huxford, and Gourisankar

Ghosh. “Protein Cofactors Are Essential for High-Affinity DNA Binding by the Nuclear Factor KB RelA Subunit.” *Biochemistry* 57, no. 20 (22 2018): 2943–57.

[36] Morgenstern, J. P., and H. Land. “Advanced Mammalian Gene Transfer: High Titre Retroviral Vectors with Multiple Drug Selection Markers and a Complementary Helper-Free Packaging Cell Line.” *Nucleic Acids Research* 18, no. 12 (June 25, 1990): 3587–96.

[37] Schröfelbauer, Bärbel, Smarajit Polley, Marcelo Behar, Gourisankar Ghosh, and Alexander Hoffmann. “NEMO Ensures Signaling Specificity of the Pleiotropic IKKβ by Directing Its Kinase Activity toward IκBα.” *Molecular Cell* 47, no. 1 (July 13, 2012): 111–21.

[38] Mruk, Dolores D., and C. Yan Cheng. “Enhanced Chemiluminescence (ECL) for Routine Immunoblotting: An Inexpensive Alternative to Commercially Available Kits.” *Spermatogenesis* 1, no. 2 (April 2011): 121–22.

[39] Zhang, Jiazhen, Kristopher Clark, Toby Lawrence, Mark W. Peggie, and Philip Cohen. “An Unexpected Twist to the Activation of IKKβ: TAK1 Primes IKKβ for Activation by Autophosphorylation.” *The Biochemical Journal* 461, no. 3 (August 1, 2014): 531–37.

[40] Nolen, B., Taylor, S., Ghosh, G., 2004. Regulation of protein kinases; controlling activity through activation segment conformation. Mol. Cell 15, 661–675.

[41] Polley, S., Passos, D.O., Huang, D.-B., Mulero, M.C., Mazumder, A., Biswas, T., Verma, I.M., Lyumkis, D., and Ghosh, G. (2016). Structural Basis for the Activation of IKK1/α. Cell Rep *17*, 1907–1914.

[42] Cordier, F., Vinolo, E., Véron, M., Delepierre, M., and Agou, F. (2008). Solution structure of NEMO zinc finger and impact of an anhidrotic ectodermal dysplasia with immunodeficiency-related point mutation. J. Mol. Biol. *377*, 1419–1432.

[43] Bagnéris, C., Ageichik, A.V., Cronin, N., Wallace, B., Collins, M., Boshoff, C., Waksman, G., and Barrett, T. (2008). Crystal structure of a vFlip-IKKgamma complex: insights into viral activation of the IKK signalosome. Mol. Cell *30*, 620–631.